Meteoritics & Planetary Science 40, Nr 1, 87–122 (2005)
Abstract available online at http://meteoritics.org

The onset of metamorphism in ordinary and carbonaceous chondrites

Jeffrey N. GROSSMAN[1*] and Adrian J. BREARLEY[2]

[1]U. S. Geological Survey, 954 National Center, Reston, Virginia 20192, USA
[2]Department of Earth and Planetary Sciences, University of New Mexico, Albuquerque, New Mexico 87131, USA
[*]Corresponding author. E-mail: jgrossman@usgs.gov

(Received May 18, 2004; revision accepted November 3, 2004)

Abstract–Ordinary and carbonaceous chondrites of the lowest petrologic types were surveyed by X-ray mapping techniques. A variety of metamorphic effects were noted and subjected to detailed analysis using electron microprobe, scanning electron microscopy (SEM), transmission electron microscopy (TEM), and cathodoluminescence (CL) methods. The distribution of Cr in FeO-rich olivine systematically changes as metamorphism increases between type 3.0 and type 3.2. Igneous zoning patterns are replaced by complex ones and Cr-rich coatings develop on all grains. Cr distributions in olivine are controlled by the exsolution of a Cr-rich phase, probably chromite. Cr in olivine may have been partly present as tetrahedrally coordinated Cr^{3+}. Separation of chromite is nearly complete by petrologic type 3.2. The abundance of chondrules showing an inhomogeneous distribution of alkalis in mesostasis also increases with petrologic type. TEM shows this to be the result of crystallization of albite. Residual glass compositions systematically change during metamorphism, becoming increasingly rich in K. Glass in type I chondrules also gains alkalis during metamorphism. Both types of chondrules were open to an exchange of alkalis with opaque matrix and other chondrules. The matrix in the least metamorphosed chondrites is rich in S and Na. The S is lost from the matrix at the earliest stages of metamorphism due to coalescence of minute grains. Progressive heating also results in the loss of sulfides from chondrule rims and increases sulfide abundances in coarse matrix assemblages as well as inside chondrules. Alkalis initially leave the matrix and enter chondrules during early metamorphism. Feldspar subsequently nucleates in the matrix and Na re-enters from chondrules. These metamorphic trends can be used to refine classification schemes for chondrites. Cr distributions in olivine are a highly effective tool for assigning petrologic types to the most primitive meteorites and can be used to subdivide types 3.0 and 3.1 into types 3.00 through 3.15. On this basis, the most primitive ordinary chondrite known is Semarkona, although even this meteorite has experienced a small amount of metamorphism. Allan Hills (ALH) A77307 is the least metamorphosed CO chondrite and shares many properties with the ungrouped carbonaceous chondrite Acfer 094. Analytical problems are significant for glasses in type II chondrules, as Na is easily lost during microprobe analysis. As a result, existing schemes for chondrule classification that are based on the alkali content of glasses need to be revised.

INTRODUCTION

Since the nineteenth century, thermal metamorphism has been recognized as an important process in the history of chondritic meteorites (e.g., Sorby 1877; see reviews by Merrill 1921; Wood 1962; Dodd 1969; Huss et al. 2004). The degree of thermal metamorphism has been an integral part of chondrite classification schemes since van Schmus and Wood (1967) introduced the concept of petrologic type and divided chondrites into types 3–6. Sears et al. (1980) recognized that type 3 ordinary chondrites showed almost as much variation in their metamorphic properties as did the entire range between types 4 and 6. Using thermoluminescence (TL) sensitivity as a strong indicator of metamorphic grade, they subdivided type 3 into ten finer divisions: types 3.0 through 3.9. This scheme, later extended to CO3 chondrites (Scott and Jones 1990; Sears et al. 1991a; Chizmadia et al. 2002), has also been used for CK3 and R3 chondrites (without published guidelines) and has been applied with somewhat less frequency to CV3 chondrites (Guimon et al. 1995; Bonal et al. 2004). Chondrites from many of the major groups show a broad range of metamorphic effects, though only the ordinary

chondrites contain members ranging from type 3.0 (the least metamorphosed) through type 6 (reheated to the point of textural integration).

It is important to fully characterize the lowest end of the metamorphic sequence displayed by chondrites for several reasons. Ideally, type 3.0 chondrites should represent material unchanged by metamorphic processes on asteroids and therefore is the most suitable for the study of nebular processes. We need to know if such meteorites exist in collections and we need accurate and quantitative methods of identifying them. For meteorites slightly affected by heating, we need to understand exactly how they have been changed in order to attempt to see through the veil of metamorphism and learn about the nebula. Weakly metamorphosed chondrites have also been affected by aqueous alteration: in some carbonaceous chondrites, this has resulted in extensive mineralogical changes, whereas in ordinary chondrites the effects are generally small (Hutchison et al. 1987; Alexander et al. 1989). In the ordinary chondrites, fluid release may have been caused by incipient metamorphic heating (Krot et al. 1997; Grossman et al. 2000), resulting in a general process of fluid-assisted metamorphism. Careful comparison of the geochemical and petrological properties of types 3.0, 3.1, and 3.2 chondrites can therefore be used to gain a more complete understanding of a variety of early asteroidal processes, including thermal processing and aqueous alteration.

The assignment of unequilibrated ordinary chondrites to petrologic types is based on a variety of parameters that vary with the degree of metamorphism. The longest known parameters, such as the degree of heterogeneity of olivine, the water and carbon content, and the amount of primordial ^{36}Ar (e.g., van Schmus and Wood 1967; Dodd et al. 1967; Zähringer 1968), as well as some parameters discovered later, including the degree of matrix recrystallization and the composition of matrix olivines (Huss et al. 1981), show broad intercorrelations, but are not sensitive enough to provide precise estimates of metamorphic grade (Sears et al. 1980). By far the most useful parameter, TL sensitivity, shows a three order of magnitude range between types 3.0 and 4, and it can be used to define a petrologic type accurate to ±0.1 for unweathered stones (Sears et al. 1980; Sears et al. 1982; Sears et al. 1991b). TL is hypothesized to track the degree to which feldspar crystallizes out of primary chondrule glass and matrix in response to metamorphism (Sears et al. 1990), although there have been no direct observations of this process in very primitive chondrites.

Thermoluminescence sensitivity alone is not sufficient for distinguishing types 3.0 and 3.1 chondrites, which show overlapping levels of induced TL and similar glow curve shapes (Sears et al. 1980; Sears et al. 1982; Benoit et al. 2002); additional observations are needed to make this distinction. DeHart et al. (1992) found that there are differences in the proportions of various types of chondrules among these low petrologic type chondrites. FeO-poor chondrules displaying yellow cathodoluminescence (CL) in their mesostasis are most abundant in type 3.0 chondrites. In addition, the Fe and Ca content of olivine and the normative mineral composition of chondrule mesostasis change during early metamorphism. Zanda et al. (1994) and Zanda (personal communication) found that P, Si, and Cr may be dissolved in some metal grains of type 3.0 chondrites, whereas during weak metamorphism to type 3.1, these elements get oxidized to form phosphates, silica, and chromite. Huss and Lewis (1994, 1995) also showed that the abundance of certain types of presolar grains decreases as weak metamorphism begins to destroy them by petrologic type 3.1.

This study presents the results of work based on a series of new observations on ordinary and CO3 chondrites drawn from systematic X-ray mapping of a wide variety of chondrites. The key observations are:

1. The distribution of Cr in silicates appears to be different in type 3.0 chondrites than in higher types. Although previous work indicated that the Cr content of olivine might be related to metamorphic grade (e.g., Dodd 1973; Ashworth 1979; McCoy et al. 1991; Johnson and Prinz 1991; DeHart et al. 1992; Jones and Lofgren 1993), this phenomenon has never been studied in detail.
2. The distribution of Na and K shows unexpected complexity in many chondrules, with the two elements apparently present in different phases and the degree of complexity related to chondrite metamorphism. It is generally assumed that the alkali elements should be contained in the same phase in chondrules, unequilibrated chondrites, and feldspar in metamorphosed ones.
3. The concentration of S in the matrix is much higher in some type 3.0 chondrites than in type 3.1 and higher-grade specimens. Dodd et al. (1967) showed that fine FeS grains were dispersed in the matrix of Krymka and Bishunpur, both currently classified as type 3.1 (an observation confirmed by Huss et al. [1981]), but no systematic study has ever been made of this effect.
4. The distribution of sulfide phases among chondrules, chondrule rims, isolated grains, and matrix appears to change during metamorphism. Similar observations have been made by Huss et al. (1981) and others, but the effects have never been quantified.

The goal in the present work is to expand on these observations in order to learn about the very earliest metamorphic processing experienced by chondrites on asteroids.

SAMPLES AND EXPERIMENTAL PROCEDURES

The X-ray mapping procedure used here was documented by Grossman et al. (2000, 2002). Mapped samples included a wide variety of weakly metamorphosed chondrites of many groups, including H, L, LL, CO, CV, CR,

and CI. Samples were mapped at either 1 μm (CO, CI, and some H chondrites) or 2 μm (L, LL, CV, CR) spatial resolution for a suite of 10 elements (Na, Mg, Al, Si, P, Ca, Cr, Mn, Fe, and Ni), in some cases supplemented by maps including K.

Four experimental protocols were used to investigate the phenomena described above: one for the investigation of the alkali element distributions in chondrule mesostases, one for the study of the chromium content of olivine, one for measuring the compositions of opaque matrix, and one for determining the distribution of sulfide minerals in chondrites. Table 1 presents a list of the samples analyzed by each protocol and the published classifications, including petrologic type, which in some cases is somewhat uncertain. In all parts of this project, the focus was on chondrites of the very lowest metamorphic grades, with samples of higher petrologic type analyzed for comparison.

Several notes should be made on the samples used in this study. Two thin sections (provided by Bunch) were analyzed as blind samples in the study of Cr distribution in olivine: Northwest Africa (NWA) 3127 and Grosvenor Mountains (GRO) 95544. NWA 3127 was a previously unclassified meteorite, though it closely resembles NWA 1756 in thin section. GRO 95544 is considered to be paired with GRO 95502, a meteorite that had already been chosen for this study. The results are presented separately for comparison. Thin sections of the three Yamato samples, Y-791324, Y-791558, and Y-793596, were all quite small in area, rendering it difficult to obtain statistically satisfactory data for studies of mesostasis and opaque matrix.

Study of Chondrule Mesostasis

Preliminary examination of X-ray maps revealed the presence of chondrules in several ordinary chondrites in which Na and K were not homogeneously distributed in mesostasis and appeared to be located in different phases. All of these chondrules were type II. Several of these chondrules were selected for further study; detailed X-ray maps for Na and K were prepared using longer count times and 1 μm/pixel resolution. Mesostasis points were selected for analysis by electron microprobe on the basis of composite Na-K X-ray maps in order to determine the compositions of the various phases that were present. Additional chondrules were identified for analysis by preparing X-ray maps of chondrules with textures similar to those already located.

In addition to microprobe analysis, a small number of CL images were obtained of chondrules in Semarkona using a single-channel photon detector attached to a JEOL 840 SEM at the U.S. Geological Survey (USGS), Reston, Virginia. Color CL images of Semarkona were also obtained using the ELN-3R luminoscope in the Department of Mineral Sciences of the National Museum of Natural History at the Smithsonian Institution.

Several demountable polished thin sections were prepared for Semarkona and Chainpur in order to perform TEM analysis of mesostasis showing heterogeneous alkali distributions. Type II chondrules in these sections were mapped in order to identify candidates for analysis. Two chondrules were located in each meteorite and were analyzed both by electron microprobe as described previously and by TEM at the University of New Mexico using the methods described by Grossman et al. (2000).

Following the characterization of mesostasis phases in Semarkona and Chainpur, a systematic survey of mesostasis in many low petrologic type chondrites was performed. Approximately 50 chondrules (or fragments of chondrules) were selected at random from each thin section. The only selection criterion was that the chondrule had to contain areas of mesostasis large enough for microprobe analysis. This eliminated all cryptocrystalline and some very fine-grained granular chondrules from the sample set. In chondrites that were finds, it also eliminated chondrules with mesostasis that is more weathered than others (type I chondrules seem to be affected the most). In each chondrule, a single analysis of mesostasis was performed away from the chondrule margin and a single analysis of the core of an olivine grain typical of the entire assemblage was obtained. If olivine was not present, a grain of low-Ca pyroxene was analyzed. This survey method was chosen to obtain thin section scale statistics on a large number of chondrules rather than detailed data on the variations that would be present in a small number of chondrules.

All microprobe analyses of mesostasis were done using the methods outlined in Grossman et al. (2002), making use of a 5 × 5 μm rastered beam, 20 nA beam current, 15 kV accelerating voltage, and completing the integration of the Na peak within 10 sec of unblanking the beam. All analyses were as free from small crystallites as possible, although in some chondrules it was not possible to avoid them all. A series of experiments was carried out under these analytical conditions to measure the Na count rate as a function of time in mesostasis from several Semarkona chondrules. Mesostasis in type I chondrules, which is generally low in Na, was relatively stable under the electron beam. Mesostasis in type II chondrules was extremely susceptible to Na loss during analysis, with most areas losing half their Na in about 20–25 sec. One area that was near albite in composition was stable under the electron beam, showing no Na loss with time. As a result of this experiment, it can be calculated that mesostasis analyses in the present work may be as much as 10% too low in Na, especially in type II chondrules where the composition does not resemble that of albite. Data were not corrected for this effect, as it was not possible to determine the exact correction necessary for each analysis. During the process of locating the analytical spot, the beam was never focused on the target area. It must be noted that prior exposure of samples to high-density electron beams (possibly by

Table 1. The meteorites analyzed for this work and the methods employed for each section. The key shows the labels used in the various figures in this paper.

Name[a]	Key	Section[b]	Class	Ref[c]	Shock[d]	Ol[e]	Meso	Matrix[f]	Image[g]
Ordinary chondrites									
Adrar 003	Adr	Mün PL 92139	L/LL3.1	Bn02	S2	I	I	X	X
Bishunpur	Bish	DTM CA-1; USNM 630-1	LL3.1	Se80	S2	I	I	X	X
Bremerörde	Bre	USNM 630-1	H/L3.7	Se83	S2	II			
Chainpur	Cha	USNM 1251-18	LL3.4	Se80	S1	I	I	X	X
Dhajala	Dha	USNM 5832-3	H3.8	Se80	S1				X
EET 90161	EET	JSC –,5	L3.0	Bn02	*S2*	I	I	X	X
GRO 95502	GRO02	JSC –,5	L3.1/3.2	Bn02	*S2*	I	I	X	X
GRO 95544	GRO44	NAU	L3.1/3.2	Bn02		II			
Krymka	Kry	USNM 1729-5	LL3.1	Se91	S3	I	I	X	X
MET 00526	MET26	JSC –,8	H3.2[h]	Bx02	S2	I	I	X	
MET 96503	MET03	JSC –,5	L3.1/3.2	Bn02	*S2*	I	I	X	X
Ngawi	Nga	USNM 2483-3a	LL3.1-3.7 br	Se90	S3	II			
NWA 1756	N56	NAU ADRC-158	LL3.0/3.2	Ru04	S1	I	I	X	
NWA 3127	N27	NAU ADRC-157	LL3.1[i]	–	S2	II			
QUE 97008	QUE	JSC –,13	L3.0	Bn02	*S2*	I	I	X	
RC 075	RC	AML-1	H3.1	Se95	S2	II			
Semarkona	Sem	USNM 1805-16	LL3.0	Se80	S2	I	I	X	X
Sharps	Sha	USNM 640-9	H3.4	Se80	S3	I	I	X	X
St Mary's County	SMC	USNM 5423-2	LL3.3	Se91	S2	I	I	X	X
Tieschitz	Tie	USNM 6783	H/L3.6	Se80	S3	I	I	X	
Y-791324	Y24	NIPR 51-3	LL3.0/3.1	Ni98	*S3*	I, II	I	X	
Y-791558	Y58	NIPR 51-3	LL3.1	Ni98	*S3*	I, II	I	X	
Y-793596	Y96	NIPR 51-3	LL3.0	Ni98		I, II	I	X	
Carbonaceous chondrites									
Acfer 094	Acf	Mün PL 93022	CC ung	Ne95	S1	II			
ALHA77307	A77	UCLA A77307,68	CO3.0	Cz02	S1	II		X	X
Colony	Col	UCLA 724 & 725	CO3.0	Cz02	S1	II		X	X
Felix	Fel	USNM 235-1	CO3.3	Cz02	S3			X	X
Isna	Isn	USNM 5890-2	CO3.8	Cz02	*S1*				X
Kaba	Kab	USNM 1052-1	CV3.1	Bo04	S1	II			
Kainsaz	Kai	USNM 2486-1	CO3.2	Cz02	S1	II		X	X
Lancé	Lan	USNM 380-1	CO3.5	Cz02	S1				X
Leoville	Leo	USNM 3535-3a	CV3.1/3.4	Bo04	S3	II			
Rainbow	Rain	USNM 6981-4	CO3.2	Cz02	*S2*	II		X	X
Vigarano	Vig	USNM 477-1	CV3.1/3.4	Bo04	S1/2	II			
Warrenton	War	USNM 43	CO3.7	Cz02	S1				X
Y-81020	Yam	NIPR 61-6	CO3.0	Cz02	S1	II		X	X

[a]Place name abbreviations: ALHA = Allan Hills; EET = Elephant Moraine; GRO = Grosvenor Mountains; MET = Meteorite Hills; NWA = Northwest Africa; QUE = Queen Alexandra Range; RC = Roosevelt County; Y = Yamato.

[b]Loaning institutions: AML = American Meteorite Laboratory; DTM = Department of Terrestrial Magnetism, Carnegie Institution of Washington; JSC = Johnson Space Center via the Antarctic Meteorite Working Group; Mün = Institut fur Planetologie, Münster; NAU = Northern Arizona University; NIPR = National Institute of Polar Research, Japan; UCLA = University of California, Los Angeles; USNM = U.S. National Museum, Smithsonian Institution.

[c]Petrologic type determined by: Se80 = Sears et al (1980); Bn02 = Benoit et al. (2002); Bx02 = Benedix et al. in Antarctic Meteorite Newsletter 25(2) (2002); Ru04 = Russell et al. (2004); Se95 = Sears et al. (1995b); Se91 = Sears et al. (1991b); Ni98 = Ninagawa et al. (1998); Se90 = Sears et al. (1990); Se83 = Sears and Weeks (1983); Cz02 = Chizmadia (2002); Ne95 = Newton et al. (1995); Bo04 = Bonal et al. (2004).

[d]Shock stages from Köblitz (2003) and Russell et al. (2004); entries in italics were determined by the first author.

[e]Analyses of random olivines and mesostasis points: I = selection of random chondrules with the sole criterion that they contain mesostasis that could be analyzed by electron probe; II = selection of random ferroan olivine grains, isolated and in chondrules, based on backscattered electron intensity (BSE) and energy-dispersive X-ray spectrometry (EDS).

[f]Matrix analyzed by rastered beam electron microprobe analysis.

[g]Distribution of sulfides and abundances of components measured by image analysis of X-ray maps.

[h]Chondrule sizes and metal abundance indicate an L or LL group classification instead of H.

[i]Classification as type 3.1 by Bunch and Wittke in part based on a pre-print of this manuscript.

previous users of a thin section) could result in inaccurate Na analyses. Included in this category are the detailed X-ray maps done in the present study to pre-characterize chondrules in Semarkona and Chainpur prior to TEM analysis. This unfortunate catch-22 could not be avoided: in order to know where to make measurements, it was necessary to examine the chondrules with a method that affected those measurements. As a result, some of the analyses of K-rich phases in Chainpur and Semarkona are probably too low in Na. However, the survey of mesostasis in the many chondrites in Table 1 should be of relatively high quality, with all data within 10% of the true values.

Study of Chondrule Olivine

In order to examine the distribution of Cr in olivine, all olivine data collected as part of the systematic study of chondrule mesostasis were compiled. Each meteorite has data for approximately 50 olivines from 50 different chondrules. To extend the study to other meteorites, a somewhat simpler selection protocol was adopted. For ordinary chondrites, one typical olivine per chondrule was again chosen, but backscatter electron (BSE) intensity and energy-dispersive X-ray spectrometry (EDS) were used to screen out forsteritic grains. For CO3 chondrites, not enough type II chondrules were present in most thin sections to provide a population of 50 grains. Consequently, isolated olivine grains were selected in addition to grains in chondrules to augment the data set. The latter method was also used for several CV3 chondrites, but these meteorites contain so little coarse-grained ferroan olivine that it was not possible to gather good statistics based on the thin sections in hand. Cr in all analyses of olivine was calculated as Cr_2O_3, although the actual oxidation state of Cr is unknown; both Cr^{2+} and Cr^{3+} may be present (Sutton et al. 1996). One meteorite sample, Meteorite Hills (MET) 96503, was selected for additional analysis. Olivine grains in several type II chondrules were examined using the JEOL JSM 6500F field emission scanning electron microscope (FESEM) at the Carnegie Institution of Washington using secondary electron and BSE imaging.

Study of Matrix

Opaque matrix was analyzed using the JEOL 8900 electron microprobe at the USGS. Areas were selected for analysis using BSE imaging and were identified on the basis of their textures. Analyzed regions were chosen to be as homogeneous-looking as possible in BSE and as free from visible grains of FeS (or other phases with grain sizes >1–2 μm) as possible. Weathering products were also avoided. A rastered beam of 30 × 30 μm (reduced in size in a few cases when necessary), 20 nA beam current and 15 kV accelerating voltage were used and data were corrected using Armstrong's (1995) CITZAF method. It is possible that some of these data require corrections for the differing densities of phases included within the analytical region, but this was not attempted for two reasons. First, the opaque matrix in most of these chondrites has not been characterized well enough to be sure of what minerals are present. Second, the grain size of the matrix in most chondrites may be small compared to the excitation volume of the electron beam, which should greatly lessen the required corrections (Warren personal communication). Ten to twenty areas of the matrix were analyzed in each chondrite, chosen to cover the entire thin section. Chondrule rim material, if it could be recognized, was avoided. Analyses that were anomalously high in S or Ni were excluded from averages on the assumption that they sampled large grains of sulfide or metal just below the surface of the thin section (never more than 10% of all analyses). Measured FeO and S were recalculated as an adjusted FeO plus FeS and the analytical total was reduced by the corresponding weight of O removed. No attempt was made to account for Fe present in Fe-Ni metal because the composition of any such metal is not known.

Image Analysis

X-ray maps of 20 chondrites collected during the preliminary phase of these investigations were studied by image analysis methods to determine the modal abundances of various components, including sulfides in differing petrographic locations. The main tool used was Adobe Photoshop supplemented by MaskPro, a plug-in written by Extensis, Inc. X-ray maps of Fe, Ni, Al, S, Mg, and Na were assembled as layers in a Photoshop image. Various selection and image masking tools were used to extract regions of each image occupied by different petrographic components (a "mask" being basically a binary or two-color image corresponding to a selected area). First, holes, cracks, and areas outside the region of the thin section were identified and masked out of the images. A mask showing metal grains was prepared by selecting pixels with high Ni and Fe but lacking S. Pixels corresponding to iron sulfides, mostly troilite, were selected on the basis of high Fe or Ni-Fe as well as S.

Selection of areas representing matrix material was considerably more difficult. This was done mainly from the Na, Al, and Mg X-ray maps, taking advantage of the fact that matrix contains less Mg than any phase in chondrules except mesostasis but lacks the high Al content of mesostasis. Matrix also often contains a distinctive Na and Al content that can be helpful in distinguishing it from chondrule minerals. At each step of the masking process by which the matrix was selected, tools for "despeckling" regions were employed to create continuous selected areas rather than porous ones. Manual corrections of selection masks were also made by painting in or erasing areas that were improperly included (e.g., areas of the matrix occurring inside chondrules, fringes around grains, and other artifacts). Following the selection of matrix, metal, and sulfide, "chondrules" were defined as all remaining silicate material. In ordinary chondrites, this is probably valid.

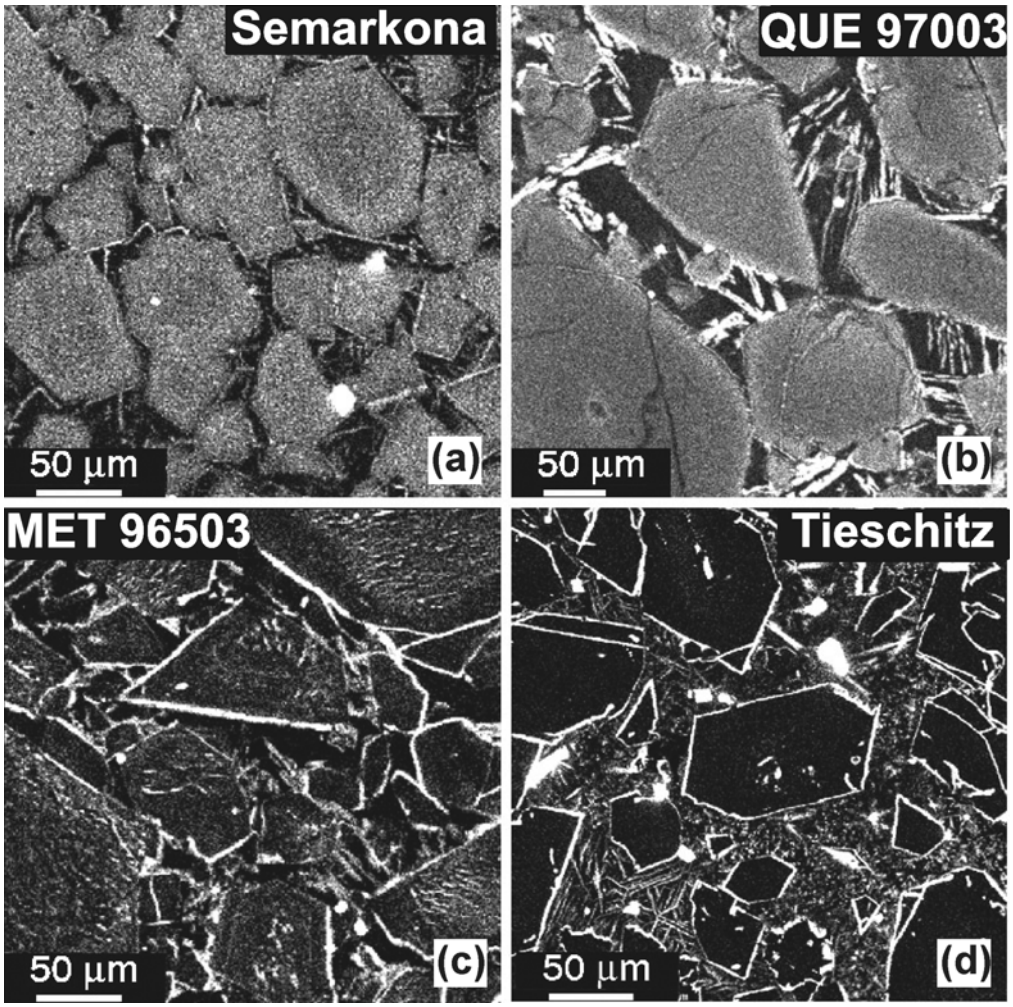

Fig. 1. Cr-Kα X-ray maps of type II chondrules in ordinary chondrites: a) in type 3.0 Semarkona, olivine (the dominant gray phase) shows igneous zoning profiles, with rims enriched in Cr over cores. Several chromite grains (bright white) are included in olivine and the mesostasis; linear bright features are clinopyroxene. b) Olivine in type 3.0 QUE 97008 resembles that in Semarkona, preserving slight core to rim igneous zoning profiles. Many small clinopyroxene grains occur in the mesostasis. c) Olivine in type 3.1/3.2 MET 96503 shows a complex distribution of Cr. Grain cores are mottled in appearance, showing what appear to be exsolution features parallel to crystallographic axes. Exteriors of olivine crystals are depleted in Cr. Bright, Cr- rich rims surround all olivine crystals. d) Olivine in type 3.6 Tieschitz is uniformly low in Cr. Inclusions of chromite are common in the olivine grains and all grains are surrounded by Cr-rich rims.

In CO3 chondrites, the chondrule fraction also includes various types of inclusions. Finally, and most importantly for this study, the sulfides were divided into three categories based on the chondrule and matrix masks: grains within chondrules, grains on the surfaces of chondrules (including all rims), and isolated assemblages and grains in the matrix.

RESULTS

The Distribution of Cr in Olivine

Preliminary X-ray mapping showed that the distribution of Cr in olivine in type II chondrules is different in ordinary chondrites of different petrologic types. In the type 3.0 chondrites (Figs. 1a and 1b), olivines in the chondrules are rich in Cr and show core-to-rim zoning profiles consistent with igneous fractionation, with Cr abundances higher near grain margins. In contrast, olivines in slightly metamorphosed types 3.1–3.2 chondrites (Fig. 1c) show a complex distribution of Cr. The cores of grains are mottled in appearance and appear to show parallel streaks of Cr-rich material oriented along crystallographic axes (as indicated by crystal faces), probably exsolution products. The outer parts of olivine grains in these meteorites are depleted in Cr, although every grain is surrounded by a very Cr-rich rim. In ordinary chondrites of petrologic type ≥3.3, olivine grains in type II chondrules appear uniformly low in Cr except for scattered, equant chromite grains in their cores, with every grain surrounded by a high-Cr rim (Fig. 1d).

Neither the Cr-rich material that is embedded in the olivine of slightly metamorphosed ordinary chondrites (Fig. 1c) nor the Cr-rich rims around olivines (Figs. 1c and

1d) were visible in BSE or secondary electron images produced by the electron microprobe. However, the exsolution products could be seen with an FESEM (Fig. 2a) as needle-like grains <50 nm wide and up to several μm long scattered throughout the cores of olivines. These grains have sizes below the resolution of the electron beam in the SEM so that all EDS spectra show extensive X-ray contributions from host olivine but with a large Cr peak. The Cr-rich rims seen around olivine grains in X-ray maps were not found using the FESEM. It is possible to detect the optical effects resulting from the presence of the Cr-rich phase in olivine using transmitted light microscopy (Fig. 2b). These are best seen using crossed polarizers and a small aperture setting. Judging from the grain size and distribution of Cr-rich needles in olivine in MET 96503 and their invisibility in microprobe BSE images, it would not be possible to do microprobe analysis of this olivine without beam overlap. Their presence would be indicated in olivine grains that show irregular zoning profiles or inhomogeneous compositions.

The variable Cr distributions in chondrites of different petrologic type are caused only by changes in the type II chondrules, which are easily recognized and resemble those documented by Jones (1990) and Jones and Lofgren (1993). Olivines in X-ray maps of type I chondrules appear to have low Cr contents regardless of petrologic type. In ordinary chondrites, there is a chemical break between olivines with compositions typical of type I and type II chondrules at around 1–3 wt% FeO (Fig. 3). Below ~2 wt% FeO, Cr_2O_3 and FeO are correlated and are apparently controlled by the same process. At low FeO content, MnO also correlates and CaO anticorrelates with FeO in olivine, implying volatility control of all the minor elements, including Cr. These correlations vanish (and the CaO-FeO anticorrelation changes to a positive correlation) above ~2 wt% FeO, and Cr_2O_3 is uniformly enriched to around 0.5 wt%. Therefore, in discussing the systematics of the Cr distribution in olivine from ordinary chondrites of different petrologic type, all grains with <2 wt% FeO were excluded. It is not certain whether this cutoff applies equally well to CO3 chondrites because data for forsteritic olivine in this group were not obtained. However, literature data from Scott and Jones (1990), Jones (unpublished data), and Brearley and Jones (1998: Fig. 30) suggest that low Cr_2O_3 concentrations only occur in low-FeO chondrules of CO3.0 chondrites as well and that the 2–3 wt% FeO cutoff is also reasonable for this chondrite group. Chromium in olivines with >2 wt% FeO does not correlate well with the other elements measured by microprobe, i.e., Mg, Al, Si, P, Ca, Ti, Mn, or Fe.

Histograms showing the distribution of Cr_2O_3 in olivine with >2 wt% FeO for 22 ordinary chondrites and 9 carbonaceous chondrites are shown in Figs. 4 and 5; average compositions of olivine are listed in Table 2. It should be noted once again that all analyses were made on material that appeared to be pure olivine in the microprobe, showing no visible signs of inclusions and having unremarkable EDS spectra. Even though some of the microprobe spots may have overlapped invisible, Cr-rich inclusions, the stoichiometry was generally excellent. In MET 96503, for example, olivines had 0.99–1.01 Si atoms per 4 oxygens, the sum of Fe, Mg, Mn, Ca, Cr, and Al was between 1.99 and 2.01; no correlations were found between formula Cr and other components.

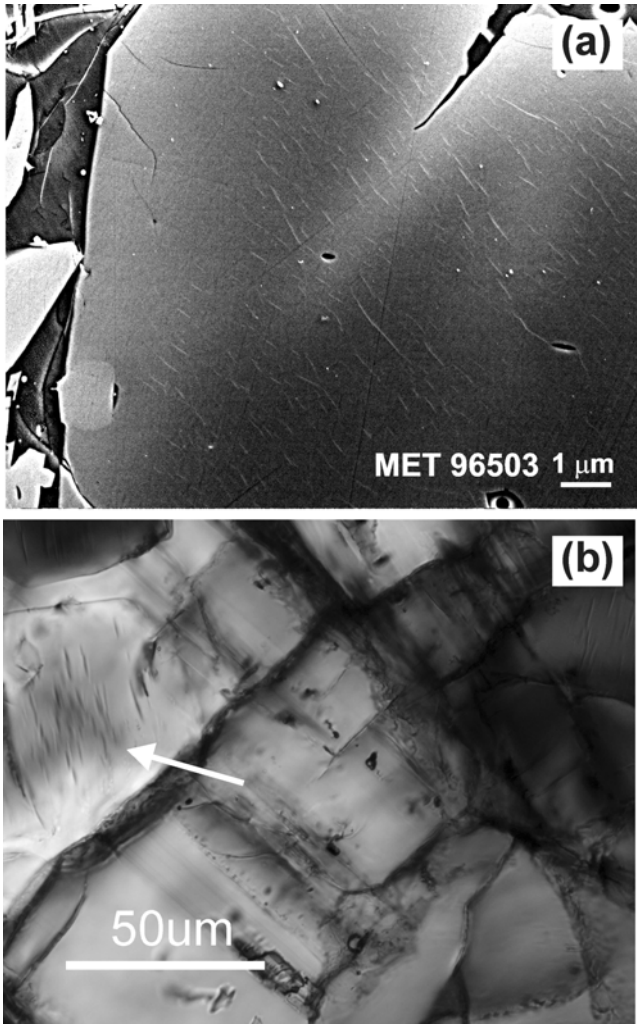

Fig. 2. Images of olivine in type II chondrules in MET 96503: a) secondary electron image taken with a field emission SEM. Numerous subparallel, needle-like grains <50 nm in width and up to several μm long occur throughout the core of the grain. The grains are absent within a few μm of the interface between olivine and mesostasis (left side). Energy dispersive X-ray spectra are consistent with these grains being chromite. No other inclusions are visible. b) Transmitted light photograph between partially crossed polarizers of a different grain than in (a). The parallel streaks visible in the grain on the left (arrow), as well as in some other grains, apparently correspond to the Cr-rich features visible in the secondary electron images.

The histograms for ordinary chondrites can be arranged in a rough sequence (Fig. 4), beginning with several

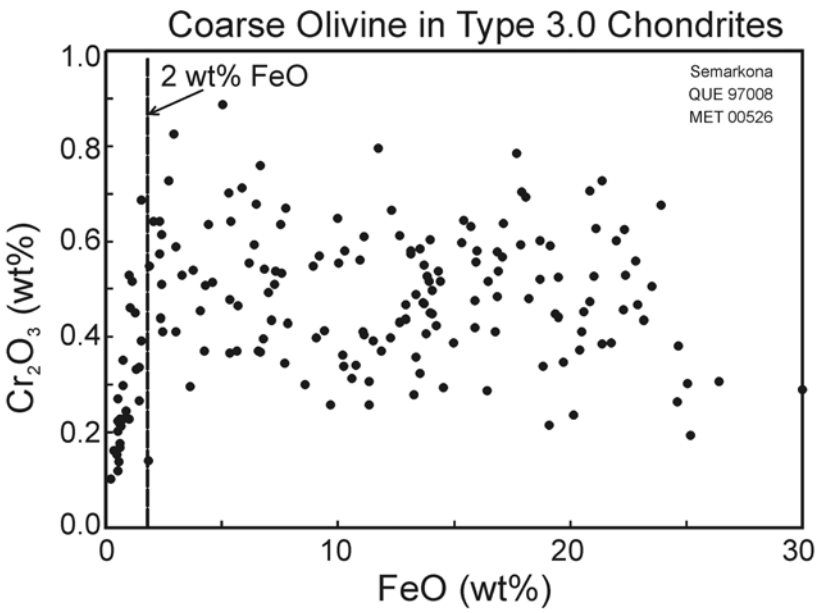

Fig. 3. Pooled microprobe data for chondrule olivine grains analyzed in three type 3.0 ordinary chondrites, Semarkona, QUE 97008, and MET 00526. Chromium is calculated as Cr_2O_3, although its actual valence state is not known. Below ~2 wt% FeO, Cr is correlated with Fe. At higher Fe contents, there is no relationship between Fe and Cr, with almost all grains containing between 0.3 and 0.7 wt% Cr_2O_3. Note that MET 00526 was initially described as type 3.2 (Table 1), but it is clearly much more primitive (see text).

meteorites in which Cr_2O_3 is mostly between 0.4 and 0.7 wt%, continuing to meteorites that show a broad distribution of Cr_2O_3 from ~0.1 to 0.8 wt%, then to a group that shows a strong mode between 0.1 and 0.25 wt% with a tail toward higher values, and ending with a group that shows only a peak below 0.2 wt%. Examination of Fig. 4 shows that this sequence is basically in accord with published petrologic types and is not related to whether the meteorite is in the H, L, or LL group. In general, meteorites classified as type 3.0 have the highest Cr_2O_3 contents in olivine, type 3.1 chondrites show the broadest distributions, and meteorites classified as type 3.2 or higher have uniformly low Cr_2O_3 in olivine. It is important to note that the published petrologic types for these meteorites are of highly variable reliability: some are thoroughly studied (e.g., Semarkona, Krymka, Bishunpur, and the other falls), some have only been analyzed for TL sensitivity, never having been studied by methods such as CL imaging (e.g., Elephant Moraine [EET] 90161, MET 96503, and Adrar 003), and others have only received a crude initial characterization (e.g., MET 00526 and NWA 1756). In the remainder of this section, the order of meteorites established in Fig. 4 will be used as a proxy for relative petrologic type for all ordinary chondrites of petrologic types 3.2 and below, supplemented by the order of literature values for meteorites of types 3.3 and higher. This point will be evaluated in the Discussion section.

Several additional observations can be drawn from Fig. 4. The paired meteorites GRO 95502 and GRO 95544 (the latter having been run as a blind sample), show identical Cr distributions in olivine. The three Yamato meteorites, Y-791324, Y-791558, and Y-793596, also show nearly identical distributions consistent with the possibility of pairing. Ngawi is a breccia composed of material ranging from petrologic types 3.1 to 3.6 or 3.7 (Sears et al. 1990; Sears et al. 1991b). Consistent with this, the distribution of Cr_2O_3 in olivine is bimodal, with a strong mode in the same range as type 3.6 Tieschitz and type 3.7 Bremervörde and a weaker mode similar to that found in type 3.0 Semarkona. There is no spatial relationship in the Ngawi thin section between chondrules with olivine in the type 3.0 range of Cr contents; these chondrules were dispersed among chondrules with low Cr in olivine, consistent with the CL images of "host" Ngawi material shown by Sears et al. (1990) and not the type 3.1 clasts in these images.

The CO3 chondrites, including their relative the ungrouped carbonaceous chondrite Acfer 094, show olivine distributions that can be arranged in a sequence similar to that of ordinary chondrites (Fig. 5). Acfer 094, a highly primitive meteorite with properties similar to CM and CO chondrites (Newton et al. 1995), which is possibly more closely related to the more matrix-rich CM group (Rubin personal communication), and two CO3.0 chondrites, ALHA77307 and Y-81020, all have olivine distributions resembling Semarkona but with somewhat lower modes around 0.3–0.4 wt% Cr_2O_3 instead of 0.5. Colony, another meteorite classified as CO3.0, shows a slightly broader distribution of Cr_2O_3 in olivine, similar to that in type 3.1 ordinary chondrites of Fig. 4. Types 3.2 Kainsaz (Sears et al. 1991a; Chizmadia et al. 2002) and Rainbow show the same olivine distributions as are found in types 3.1–3.2 ordinary chondrites, with a peak around 0.1 wt% Cr_2O_3.

Of the five analyzed CV3 chondrites, only three thin

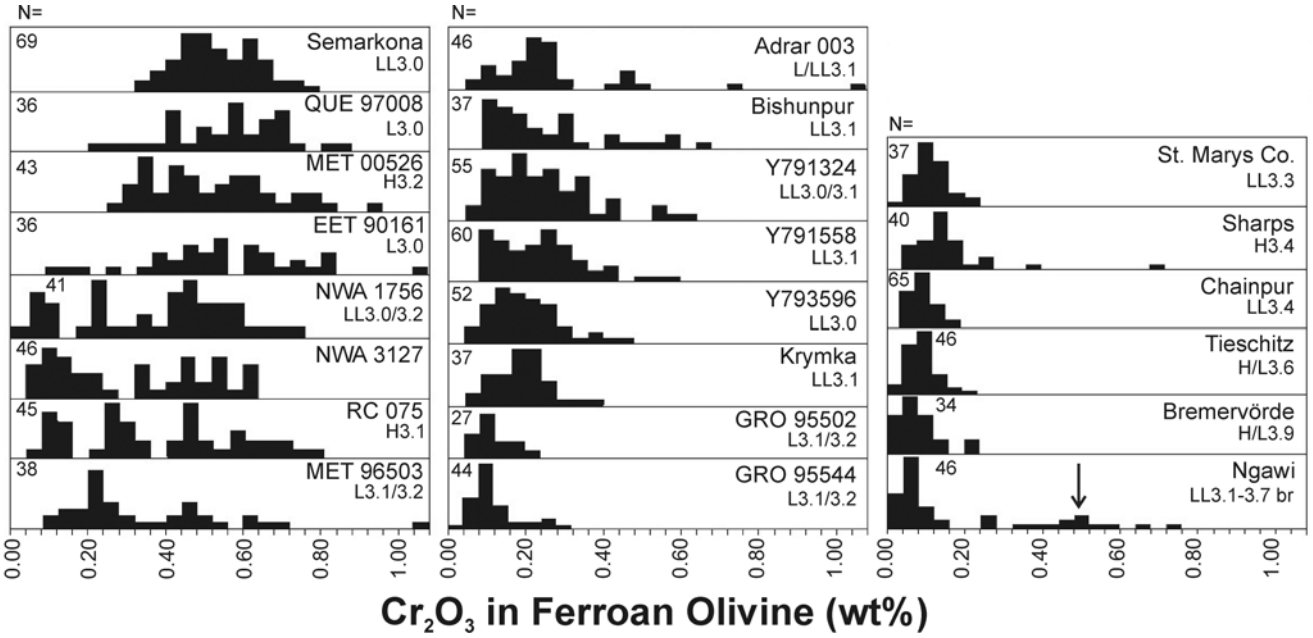

Fig. 4. Histograms showing the distribution of Cr_2O_3 in olivine from 22 unequilibrated ordinary chondrites. All olivine grains with <2 wt% FeO were excluded; every analysis represents a different chondrule. The meteorites are arranged in a sequence according to the shapes of the histograms starting with Semarkona in the upper left and moving downwards from left to right across the figure. Ngawi, which is known to be a breccia of low and high petrologic type material, was arbitrarily placed at the lower right (an arrow points to the peak in the distribution corresponding to low petrologic type grains). The number of analyses is shown at the left of each histogram. The petrologic type taken from the literature (Table 1) is also indicated.

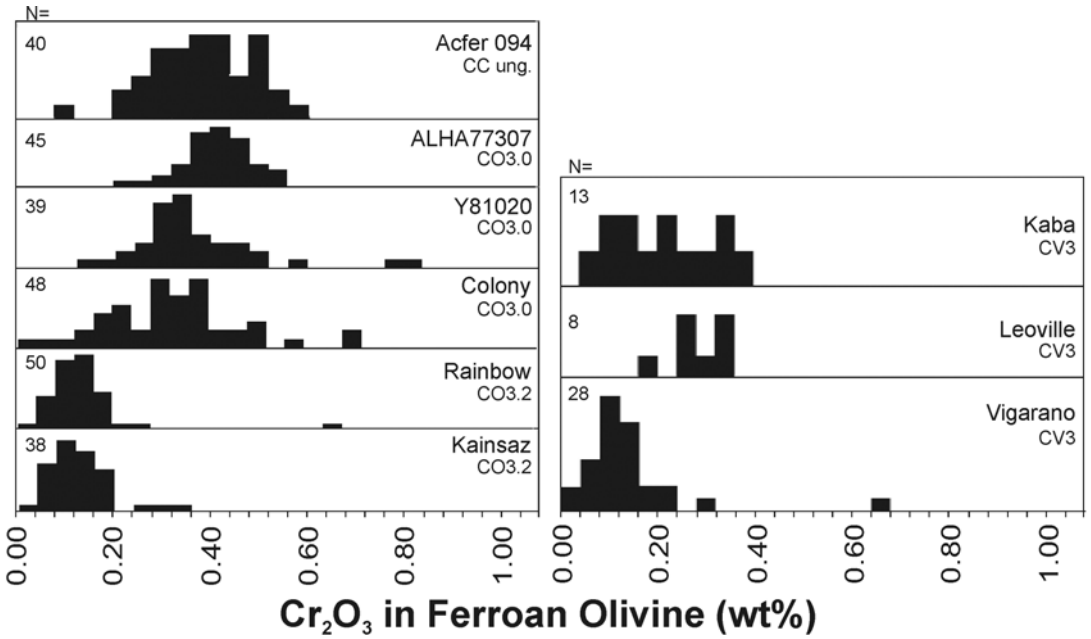

Fig. 5. Histograms showing the distribution of Cr_2O_3 in olivine from five CO3 chondrites, Acfer 094, an ungrouped carbonaceous chondrite related to the CM and CO group, and 3 CV3 chondrites. All olivine grains with <2 wt% FeO were excluded; every analysis represents a different chondrule or isolated grain. Histograms for CO3 chondrites are arranged as in Fig. 4.

Table 2. Mean compositions of coarse-grained (non-matrix) ferroan olivine (wt%). All grains with <2 wt% FeO have been excluded. Samples are arranged in approximate order of metamorphic grade as determined in this work.

Meteorite	N	MgO	Al_2O_3	SiO_2	P_2O_5	CaO	TiO_2	Cr_2O_3	MnO	FeO	Total	Fa (mol%)	Meth[a]
Ordinary chondrites													
Semarkona	69	46.7 ± 5.1	0.02 ± 0.03	39.5 ± 1.6	0.03 ± 0.03	0.15 ± 0.08	0.01 ± 0.01	0.50 ± 0.10	0.43 ± 0.17	12.6 ± 6.2	100.0	13.3 ± 6.7	I
QUE 97008	36	44.7 ± 5.6	0.04 ± 0.04	38.6 ± 1.7	0.04 ± 0.05	0.19 ± 0.08	0.01 ± 0.02	0.52 ± 0.15	0.44 ± 0.19	13.7 ± 6.5	98.2	15.0 ± 7.5	I
MET 00526	43	44.7 ± 6.3	0.03 ± 0.02	40.0 ± 3.1	0.04 ± 0.06	0.17 ± 0.08	0.01 ± 0.02	0.47 ± 0.16	0.50 ± 0.22	13.2 ± 7.0	99.1	14.5 ± 8.2	I
EET 90161	37	45.5 ± 5.3	0.03 ± 0.03	39.7 ± 1.2	0.02 ± 0.03	0.17 ± 0.07	0.02 ± 0.02	0.50 ± 0.21	0.50 ± 0.17	12.7 ± 6.0	99.2	13.8 ± 7.0	I
NWA 1756	41	44.0 ± 7.3	0.02 ± 0.03	38.0 ± 1.7	0.03 ± 0.04	0.15 ± 0.08	0.01 ± 0.02	0.33 ± 0.20	0.43 ± 0.17	14.5 ± 8.5	97.6	16.1 ± 10.1	I
NWA 3127	46	44.1 ± 4.9	0.02 ± 0.03	39.3 ± 1.1	0.03 ± 0.03	0.14 ± 0.07	0.01 ± 0.02	0.28 ± 0.19	0.37 ± 0.12	15.7 ± 5.6	99.9	16.8 ± 6.7	II
RC 075	45	45.9 ± 5.5	0.03 ± 0.04	38.6 ± 1.7	0.02 ± 0.02	0.15 ± 0.08	0.02 ± 0.03	0.34 ± 0.20	0.38 ± 0.21	12.4 ± 6.2	97.8	13.4 ± 7.1	II
MET 96503	39	43.5 ± 5.9	0.03 ± 0.02	38.5 ± 1.6	0.03 ± 0.04	0.17 ± 0.07	0.01 ± 0.02	0.31 ± 0.22	0.53 ± 0.20	14.4 ± 6.5	97.5	16.0 ± 7.8	I
Bishunpur	37	44.0 ± 6.0	0.04 ± 0.06	39.2 ± 1.2	0.03 ± 0.04	0.17 ± 0.06	0.02 ± 0.03	0.22 ± 0.16	0.53 ± 0.25	13.9 ± 6.9	98.1	15.4 ± 8.1	I
Adrar 003	47	45.8 ± 6.0	0.02 ± 0.03	39.7 ± 1.3	0.02 ± 0.03	0.16 ± 0.06	0.02 ± 0.02	0.23 ± 0.21	0.41 ± 0.19	11.8 ± 6.9	98.2	13.0 ± 8.1	I
Y-791324	55	44.9 ± 5.6	0.02 ± 0.03	39.3 ± 1.2	0.03 ± 0.05	0.15 ± 0.08	0.02 ± 0.02	0.21 ± 0.13	0.41 ± 0.14	14.3 ± 6.6	99.4	15.4 ± 7.6	I,II
Y-791558	60	44.6 ± 6.1	0.02 ± 0.02	39.1 ± 1.4	0.03 ± 0.04	0.15 ± 0.07	0.01 ± 0.02	0.20 ± 0.12	0.45 ± 0.16	14.5 ± 6.9	99.0	15.8 ± 8.2	I,II
Y-793696	52	42.6 ± 5.2	0.02 ± 0.03	38.9 ± 1.3	0.05 ± 0.08	0.17 ± 0.07	0.01 ± 0.02	0.16 ± 0.09	0.43 ± 0.12	17.4 ± 6.0	99.8	18.9 ± 7.1	I,II
Krymka	37	45.5 ± 5.2	0.03 ± 0.02	37.9 ± 1.6	0.02 ± 0.04	0.20 ± 0.13	0.02 ± 0.02	0.15 ± 0.07	0.43 ± 0.15	13.3 ± 6.1	97.6	14.3 ± 7.0	I
GRO 95502	27	43.4 ± 6.3	0.02 ± 0.03	37.7 ± 1.5	0.04 ± 0.05	0.17 ± 0.07	0.01 ± 0.02	0.08 ± 0.05	0.49 ± 0.20	15.9 ± 7.2	97.8	17.4 ± 8.4	I
GRO 95544	44	44.8 ± 4.5	0.02 ± 0.03	39.6 ± 1.1	0.03 ± 0.03	0.13 ± 0.07	0.01 ± 0.02	0.08 ± 0.06	0.37 ± 0.10	14.5 ± 5.1	99.5	15.5 ± 5.9	II
St Mary's County	37	45.3 ± 6.5	0.02 ± 0.01	39.3 ± 1.7	0.04 ± 0.10	0.13 ± 0.06	0.01 ± 0.02	0.08 ± 0.04	0.42 ± 0.19	13.1 ± 7.3	98.4	14.3 ± 8.5	I
Sharps	40	44.9 ± 5.6	0.03 ± 0.03	39.7 ± 1.3	0.03 ± 0.04	0.15 ± 0.06	0.02 ± 0.02	0.12 ± 0.11	0.37 ± 0.16	14.1 ± 6.5	99.4	15.2 ± 7.5	I
Chainpur	65	42.0 ± 7.6	0.02 ± 0.02	39.0 ± 1.6	0.03 ± 0.04	0.14 ± 0.08	0.02 ± 0.02	0.06 ± 0.04	0.44 ± 0.16	17.4 ± 8.7	99.1	19.4 ± 10.4	I
Tieschitz	46	42.3 ± 8.4	0.02 ± 0.02	39.1 ± 2.0	0.04 ± 0.06	0.15 ± 0.06	0.01 ± 0.02	0.05 ± 0.04	0.45 ± 0.22	17.3 ± 9.6	99.5	19.4 ± 11.7	I
Bremervörde	34	44.9 ± 3.5	0.02 ± 0.02	39.4 ± 0.7	0.01 ± 0.01	0.06 ± 0.05	0.03 ± 0.04	0.05 ± 0.05	0.42 ± 0.10	15.7 ± 3.9	100.6	16.5 ± 4.4	II
Ngawi	46	38.4 ± 5.0	0.01 ± 0.01	37.3 ± 2.1	0.03 ± 0.03	0.08 ± 0.07	0.01 ± 0.02	0.15 ± 0.20	0.43 ± 0.08	20.9 ± 6.1	97.4	23.6 ± 7.3	II
CO3 chondrites and Acfer 094													
Acfer 094	40	32.7 ± 4.4	0.04 ± 0.03	36.8 ± 1.1	0.05 ± 0.08	0.30 ± 0.12	0.02 ± 0.02	0.34 ± 0.10	0.33 ± 0.07	28.5 ± 4.9	99.1	33.1 ± 7.0	II
ALHA77307	45	32.2 ± 5.4	0.04 ± 0.02	36.4 ± 1.2	0.02 ± 0.03	0.24 ± 0.12	0.03 ± 0.03	0.38 ± 0.07	0.31 ± 0.08	27.3 ± 6.4	96.9	32.5 ± 8.8	II
Y-81020	39	32.7 ± 7.2	0.04 ± 0.03	36.5 ± 1.6	0.04 ± 0.04	0.23 ± 0.11	0.02 ± 0.03	0.33 ± 0.13	0.33 ± 0.13	27.3 ± 8.3	97.5	32.5 ± 11.9	II
Colony	27	28.6 ± 9.9	0.05 ± 0.05	36.1 ± 2.2	0.04 ± 0.04	0.20 ± 0.07	0.01 ± 0.02	0.31 ± 0.13	0.36 ± 0.10	32.1 ± 11.4	97.7	39.8 ± 15.5	II
Rainbow	49	30.9 ± 6.0	0.04 ± 0.02	36.6 ± 1.3	0.03 ± 0.04	0.18 ± 0.07	0.01 ± 0.02	0.08 ± 0.05	0.32 ± 0.08	31.0 ± 7.0	99.1	36.5 ± 10.2	II
Kainsaz	41	34.2 ± 7.1	0.04 ± 0.03	37.0 ± 1.6	0.03 ± 0.05	0.16 ± 0.08	0.02 ± 0.03	0.09 ± 0.06	0.28 ± 0.08	26.5 ± 8.1	98.4	30.9 ± 11.1	II
CV3 chondrites													
Kaba	13	29.8 ± 3.4	0.04 ± 0.03	36.7 ± 0.7	0.04 ± 0.04	0.35 ± 0.26	0.02 ± 0.03	0.17 ± 0.10	0.34 ± 0.06	32.1 ± 3.7	99.5	37.8 ± 5.4	II
Leoville	8	38.7 ± 4.0	0.04 ± 0.03	37.9 ± 1.0	0.03 ± 0.06	0.22 ± 0.09	0.01 ± 0.01	0.24 ± 0.05	0.27 ± 0.09	21.7 ± 4.2	99.0	24.0 ± 5.3	II
Vigarano	36	35.8 ± 7.9	0.03 ± 0.02	37.5 ± 1.6	0.03 ± 0.05	0.17 ± 0.07	0.02 ± 0.03	0.10 ± 0.11	0.29 ± 0.09	25.7 ± 9.0	99.6	29.3 ± 11.5	II
Bali	4	40.0 ± 4.5	0.06 ± 0.04	37.8 ± 0.2	0.06 ± 0.03	0.21 ± 0.08	0.02 ± 0.02	0.24 ± 0.15	0.26 ± 0.03	20.4 ± 3.8	99.0	22.4 ± 5.4	II
Allende	3	29.3 ± 2.7	0.05 ± 0.02	36.3 ± 0.8	0.01 ± 0.01	0.22 ± 0.02	0.04 ± 0.01	0.07 ± 0.03	0.31 ± 0.03	32.0 ± 2.8	98.3	38.0 ± 4.3	II

[a]Method of selecting grains: I = selection of random chondrules with the sole criterion of their containing mesostasis that could be analyzed by electron probe; II = selection of random ferroan olivine grains, isolated and in chondrules, based on backscattered electron intensity.

sections contained enough coarse-grained ferroan olivine to produce a statistically meaningful distribution (Fig. 5). The olivine histogram in Vigarano resembles those of the CO3.2 chondrites, Kainsaz and Rainbow. Kaba and Leoville seem to show broader distributions, but the statistics are not good enough to show whether they are more like type 3.0 or 3.1 ordinary chondrites. Only three grains were analyzed in Allende and all had low Cr_2O_3 (Table 2).

Alkali Distribution in Chondrule Mesostasis

X-Ray Mapping Studies

It is generally assumed that the alkalis, including Na and K, behave as incompatible elements in chondrule melts and therefore would be concentrated in residual glass formed after the crystallization of mafic silicate minerals. This fact, plus their similar volatility, should result in a high degree of chemical coherence between Na and K. Because of these assumptions and the low cosmic abundance of K, little attention has been paid to this element in the chondrule literature. In primitive chondrites such as Semarkona, no significant alkali-bearing phases other than glass have been identified in chondrules, with the exception of plagioclase in rare Al-rich chondrules. It was therefore surprising when examination of Na and K X-ray maps of ordinary chondrites revealed regions of mesostasis rich in K and other regions rich in Na in some otherwise unremarkable type II chondrules. High resolution images derived from BSE and X-ray maps of five of these chondrules from Semarkona, Chainpur, and Sharps are shown in Fig. 6. It was not possible to distinguish between Na- and K-rich mesostasis using BSE images or optical microscopy; only very subtle differences could be detected in places where a boundary between the two materials was known to exist based on X-ray maps.

In chondrules containing both types of mesostasis, K-rich material occurs in a variety of petrographic locations, some consistent from chondrule to chondrule and others not (Table 3). Mesostasis inclusions trapped inside olivine crystals, as well as embayments in olivine crystals are almost invariably rich in K (visible in Figs. 6a, 6b, 6d, and 6e). Areas of mesostasis that are tightly sandwiched between olivine crystals also tend to be rich in K (most noticeable in Fig. 6a). In some cases, K-rich mesostasis is concentrated near the core of the chondrule (Figs. 6a and 6d); in other cases it occurs mostly near the surface of the chondrule (Fig. 6b) or it may be scattered throughout the chondrule (Figs. 6c and 6e). The proportion of K-rich to Na-rich mesostasis is highly variable (Table 3; compare Figs. 6c and 6e).

There is a relationship between mesostasis composition and CL intensity in chondrules with inhomogeneous alkali distributions. Semarkona chondrule 7-4 shows bright blue CL, typical of many FeO-rich chondrules in type 3 ordinary chondrites. Figure 6f demonstrates that the CL emanates only from the Na-rich mesostasis, with K-rich areas being entirely nonluminescent.

The abundance of chondrules displaying inhomogeneous alkali distributions increases with petrologic type. After the discovery of a single such chondrule in an X-ray map of type 3.0 Semarkona, many other chondrules had to be surveyed to find other examples. Conversely, nearly every type II chondrule in type 3.4 Chainpur and Sharps seemed to have this property.

Mineralogy

Average analyses of coexisting Na-rich and K-rich mesostasis in eight chondrules (three from Semarkona, four from Chainpur, and one from Sharps) are listed in Table 4. Areas to be analyzed were selected on the basis of X-ray maps prepared earlier, the only available method for distinguishing these materials. Unfortunately, K-rich mesostasis is highly beam sensitive, being susceptible to Na loss (see the Experimental Methods section; note the hatched area in Fig. 6e). It is likely that the Na contents of K-rich mesostasis listed in Table 4 are too low. The Na-rich areas in Semarkona and Chainpur chondrules have compositions near pure albite, with ~70–80 wt% normative albite, 10–15 wt% normative pyroxene, and a small amount of normative quartz and other minerals. Potassium contents are near detection limits, generally <0.1 wt% K_2O. The Na-rich mesostasis in the Sharps chondrule is also albitic, but contains much more normative pyroxene. K-rich mesostasis also contains substantial amounts of normative albite despite beam damage, ranging from ~30 to 60 wt%. K_2O contents of the latter material are ~1.0 wt% in Semarkona and 1.6–1.8 wt% in Chainpur and Sharps, resulting in normative orthoclase contents of ~6 wt% in Semarkona and ~10 wt% in the other meteorites. The K-rich mesostasis analyses also show high normative quartz and corundum, probably artifacts produced by Na-loss during analysis (see the Discussion section).

TEM analyses were performed on two Semarkona and two Chainpur chondrules to identify the phases present in Na-rich and K-rich mesostasis. Results are similar for the two meteorites. K-rich mesostasis areas are composed of K-rich, feldspathic glass (Fig. 7a). Embedded in the glass are abundant crystallites of clinopyroxene, Fe oxides, and other minerals such as chromite and phosphates. Na-rich mesostasis areas are dominated by crystalline albitic feldspar (Figs. 7b and 7c), commonly intergrown with clinopyroxene resembling that in K-rich areas. EDS analyses show that the albite contains several wt% FeO and MgO. In some areas of Semarkona chondrules, there is evidence of aqueous alteration of the K-rich glass (Fig. 7a). One area showed abundant smectite as well as a Si-rich glass (Fig. 7d); however, aqueous alteration effects are in general minor and are probably superimposed on the chondrule assemblage of K-rich glass plus crystalline feldspar.

Surveys of Mesostasis Compositions

Several observations from the initial study of Semarkona and Chainpur chondrules with inhomogeneous alkali

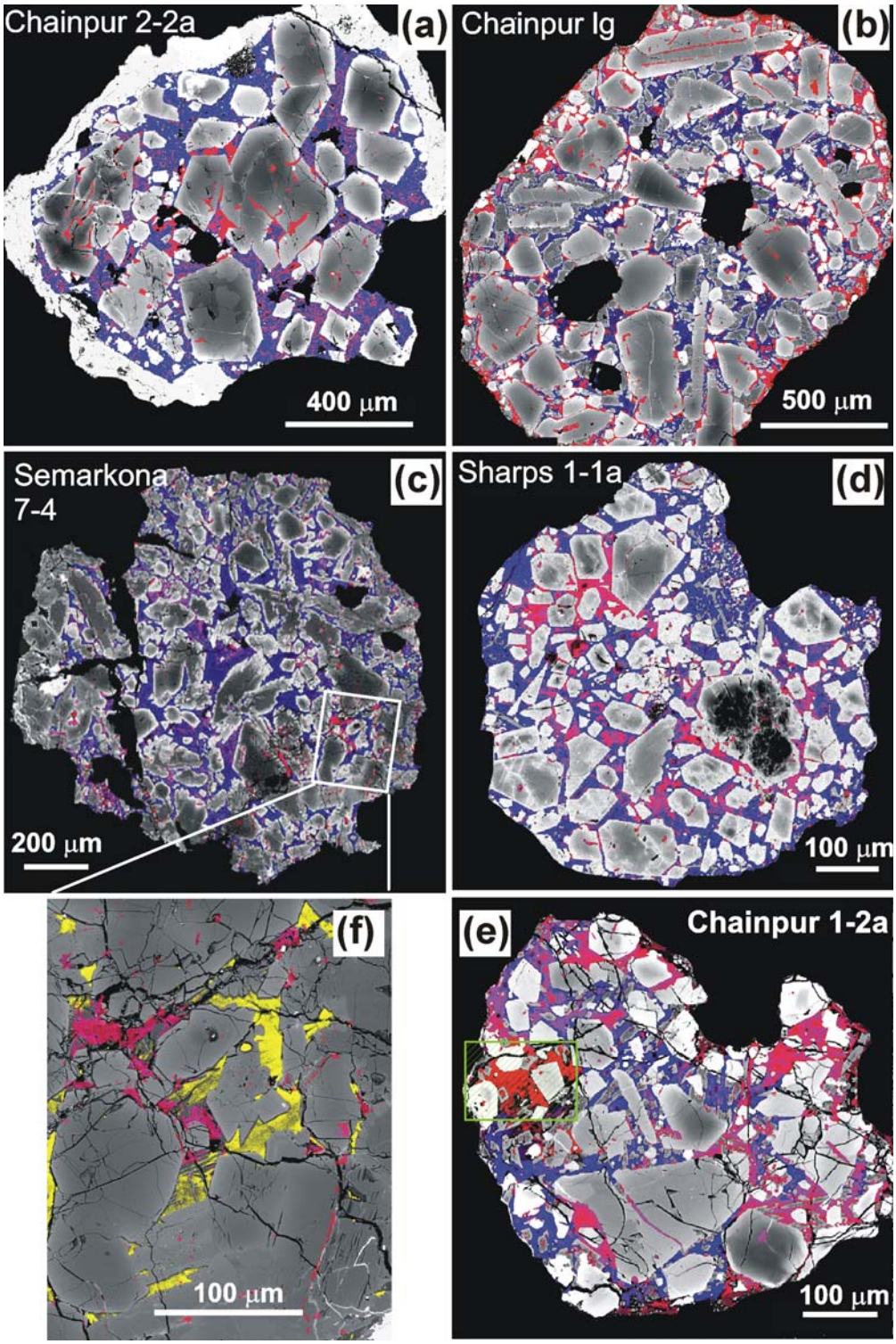

Fig. 6. Images of type II chondrules in ordinary chondrites that contain heterogeneous distributions of alkali elements. The black-and-white portion of each photograph is a backscattered electron image. In (a) through (e), X-ray maps of Na and K have been shaded blue and red, respectively, and digitally combined with the BSE image to produce a composite in which only chondrule mesostasis appears in color, with the shade indicating whether the mesostasis is rich in Na or K. In (f), the same process was followed, except in this case red corresponds to intensities in the K X-ray map and yellow represents areas showing bright cathodoluminescence. Regions high in K and bright in cathodoluminescence would appear orange. All of the yellow areas in the image correspond to Na-rich mesostasis. The green hatched region in (e) covers an area that received prolonged exposure to the electron beam of the microprobe, resulting in the loss of most of the Na.

Table 3. Distribution of potassium-rich mesostasis in type II chondrules with inhomogeneous alkali distributions in mesostasis.

Sample	% Mesostasis K-rich	% Mesostasis Na-rich	K-rich glass inclusions	Narrow K-rich areas	Bulk of K-rich mesostasis		
					Central	Peripheral	Dispersed
Semarkona 7-4	10	90	Y	Y			X
Semarkona 2x-2	40	60	Y	n/a	X		
Semarkona 8x-1	5	95	Y	Y	X		
Chainpur 1-2a	40	60	Y	N			X
Chainpur 2-2a	15	85	Y	Y	X		
Chainpur 3x-1	10	90	Y	Y		X	
Chainpur 4x-1	10	90	Y	?	X		
Chainpur 4x-2	<5	>95	Y	N			X
Chainpur 4x-4	90	10	Y	n/a			X
Chainpur Lg	20	80	Y	Y		X	
Sharps 1-1a	20	80	Y	Y	X		

distributions required further investigation. Is the observed difference in abundance of these chondrules between type 3.0 and 3.4 due to metamorphism? What is the true composition of glassy, K-rich mesostasis prior to degradation under the electron beam? Is the higher K_2O content of K-rich mesostasis in Chainpur compared to that in Semarkona a metamorphic effect? Are inhomogeneous alkali distributions really limited to type II chondrules? To investigate these questions, mesostasis compositions were surveyed in a large suite of low-petrographic-type ordinary chondrites. Although X-ray mapping was done on some of the thin sections prior to this survey, the maps were thin section wide and the beam exposure was too brief to significantly alter the compositions of susceptible phases.

Figure 8 shows the results of the mesostasis survey presented as alkali abundances normalized to Al and to CI chondrites. Points are classified according to the Fe content of coexisting mafic silicate minerals. A slightly different cutoff in FeO content between the chondrule groups was used here than for the Cr discussion above: 3 wt% FeO (Fa_3 olivine) instead of 2 wt%, to slightly improve the statistics of the lowest-Fe group. Points plotting near 1.6 on the Na axes in Fig. 8 represent material similar to the Na-rich mesostasis described above for Chainpur and Semarkona chondrules with inhomogeneous alkali distributions. These do occur with increasing frequency in the sequence of the plots (based on the Cr distribution of olivine), almost exclusively in chondrules with olivine above Fa_3, and preferentially in chondrules with olivine above Fa_{10}. Most of this increase seems to occur above petrologic type 3.3 starting with St Mary's County and Chainpur and continuing with Sharps (not shown).

All of the chondrites in Fig. 8 contain a significant population of mesostasis with K/Na above solar (above the diagonal lines) and with Na/Al > 1. In Semarkona and Chainpur, these populations have similar K/Al ratios to those found in K-rich mesostasis listed in Table 4, but at higher Na/Al, presumably because they were analyzed without beam-induced loss of Na (the plot for Semarkona also shows three points at lower Na/Al that could be real, but also could reflect prior beam damage to this well-studied thin section, possibly by the first author). The mean K/Al ratio of this population of mesostasis increases in the order of the plots. To quantify this, chondrules were selected that contain olivine above Fa_{10} (the crosses in Fig. 8) and that also have K/Al above 0.6 × CI and Na/Al above 0.5. This excludes all chondrules that might have affinities to type I and also excludes the Na-rich mesostasis associated with crystalline albite. Averages of mesostasis in the remaining chondrules are listed in Table 5 and for most chondrites encompass 15–20 analyses. Mean K/Al in these chondrules anticorrelates with mean Cr_2O_3 in ferroan olivine from the same meteorites (Fig. 9a), with the data defining three rough groups. Semarkona has by far the lowest K/Al; the three other meteorites with high Cr_2O_3 in olivine also have low mean K/Al in these chondrules. Not much variation in K/Al is seen within a second group with intermediate Cr_2O_3 content in olivine. The three meteorites known to be of petrologic types 3.3 and 3.4 have very potassic mesostases, low Cr_2O_3 in olivine, and form a third grouplet. The MnO and FeO contents of this population of K-rich mesostases also seem to correlate with Cr_2O_3 in olivine (Table 5).

The mesostasis survey also revealed major changes in alkali distribution in chondrules with low FeO in mafic silicates (type I chondrules). These trends have been observed before (e.g., DeHart et al. 1992). The black dots in Fig. 8, representing chondrules with olivine below Fa_3, cluster near the origin in Semarkona and move to higher alkali contents along the sequence of the plots. Average compositions of mesostasis in these chondrules are given in Table 6. The Na/Al ratio varies by a factor of 5 and K/Al by a factor of 10 across the sequence (ignoring meteorites having <4 analyses, for which statistics are unreliable). As was seen above for K-rich mesostasis in ferroan chondrules, MnO decreases along the plot-sequence in this population of chondrules as well, although FeO is fairly constant. The relationship between the mean Na/Al ratio of mesostasis in chondrules with olivine below Fa_3 and the mean Cr_2O_3 in ferroan olivine in the same chondrites is shown in Fig. 9b. Note that these two parameters were measured in very

Table 4. Compositions of coexisting areas of Na-rich and K-rich mesostasis in chondrules from Semarkona, Chainpur, and Sharps. Also shown are CIPW normative mineral compositions[a]. All data in wt%.

Comment	Type	Na_2O[b]	MgO	Al_2O_3	SiO_2	P_2O_5	Cl	K_2O	CaO	TiO_2	Cr_2O_3	MnO	FeO	Total[c]	Q	Or	Ab	An	Co	Pyx	Other
Sem 2x-2	Na	9.84	1.06	15	64	0.46	0.01	0.07	0.62	0.39	0.02	0.06	4.45	96	2	0.4	80	0	0	12	5
Sem 2x-2	K	3.5	1.14	13.5	69.5	0.52	0.00	0.99	0.32	0.51	0.04	0.15	5.73	95.9	42	6	31	0	8	13	0.4
Sem 8x-1	Na	9.46	1.53	14.4	67.9	0.28	0.02	0.07	1.07	0.38	0.05	0.1	5.05	100.3	6	0.4	74	0	0	16	4
Sem 8x-1	K	2.98	1.2	13.2	73.6	0.49	0.02	1.01	0.69	0.46	0.06	0.13	4.95	98.8	47	6	26	0.2	7	72	2
Sem 7-4	Na	8.63	0.96	17.9	66.4	0.09	0.00	0.3	2.61	0.47	0.02	0.12	2.53	99.9	7	1.8	73	9	0	8	1
Sem 7-4	K	4.19	1.19	15.7	72.8	0.1	0.01	1.11	1.17	0.58	0.07	0.11	2.67	99.7	38	7	36	5	6	7	1
Chainpur 4x-1	Na	10.6	1.32	15.7	68	0.33	0.02	0.05	0.91	0.57	0.03	0.04	2.4	100	3	0.3	80	0	0	10	6
Chainpur 4x-1	K	7.66	0.77	14.5	70.2	0.26	0.03	1.6	1.27	0.56	0.12	0.07	2.96	100	15	10	65	0.4	0	8	2
Chainpur 3x-1	Na	10.1	1.42	15.4	68.1	0.2	0.01	0.02	1.24	0.52	0.02	0.04	2.9	100	5	0.1	79	0	0	12	4
Chainpur 3x-1	K	6.83	1.03	15	70.8	0.16	0.04	1.79	0.92	0.47	0.06	0.09	2.85	100	19	11	58	4	0.5	7	1
Chainpur 4x-4	Na	10.1	1.17	15	69.3	0.28	0.02	0.09	0.94	0.51	0.04	0.03	2.48	100	7	0.5	77	0	0	10	6
Chainpur 4x-4	K	7.71	0.88	14.1	72.3	0.23	0.04	1.62	0.49	0.54	0.02	0.04	2.11	100	19	10	63	0	0	6	2
Chainpur 1-2a	Na	9.46	2.66	15.5	63.8	1.2	0.04	0.06	1.37	0.51	0.06	0.07	5.4	100	1	0.4	79	0	0.4	16	3
Chainpur 1-2a	K	6.63	1.2	13.6	70.5	1.21	0.06	1.8	1.91	0.54	0.05	0.04	2.43	100	21	11	56	2	0.2	7	4
Sharps 1-1a	Na	6.77	3.85	11	58.7	1.93	0.00	0.2	8.43	0.44	0.07	0.24	8.32	100	0	1.2	56	0	0	37	6
Sharps 1-1a	K	4.55	5.24	10.2	58	1.3	0.05	1.57	10.5	0.45	0.1	0.2	7.89	100	1	9	39	3	0	44	4

[a]Normative components are Q = quartz; Or = orthoclase; Ab = albite; An = anorthite; Co = corundum; Pyx = all pyroxene components.

[b]Na_2O contents of all K-rich phases are probably too low due to loss of Na under the electron beam.

[c]Data for Chainpur and Sharps were normalized to 100% from slightly higher values of 102–104%.

Table 5. Mean compositions of mesostasis in randomly selected chondrules with coexisting olivine compositions of $Fa_{>10}$. Analyses with Na/Al < 0.5 ×CI and with K/Al < 0.6 × CI (volatile-poor and albitic mesostases, respectively) were excluded. One point analyzed per chondrule.

Meteorite	N	Na_2O	MgO	Al_2O_3	SiO_2	P_2O_5	Cl	K_2O	CaO	TiO_2	Cr_2O_3	MnO	FeO	Total	Fa (ol)	Na/Al_{CI}	K/Al_{CI}
Semarkona	40	6.9	1.54	13.8	67.4	0.45	0.01	0.81 ± 0.15	2.56	0.47	0.07	0.22	6.39	100.6	16.9	1.22	1.43
QUE 97008	21	6.9	1.59	13.2	66.5	0.59	0.01	1.04 ± 0.13	2.15	0.55	0.07	0.28	6.53	99.4	18.1	1.29	1.92
MET 00526	20	7.6	1.80	13.8	64.4	0.66	0.02	1.03 ± 0.14	1.93	0.48	0.07	0.24	6.45	98.5	19.1	1.36	1.82
EET 90161	17	7.3	2.65	12.2	68.1	0.41	0.02	0.97 ± 0.27	2.71	0.47	0.11	0.23	5.71	100.9	19.2	1.47	1.93
NWA 1756	20	7.4	2.33	12.7	62.9	0.57	0.01	1.08 ± 0.39	2.36	0.46	0.27	0.22	6.69	97.0	22.5	1.44	2.09
MET 96503	21	8.1	1.73	12.9	66.2	0.43	0.01	1.21 ± 0.11	1.95	0.49	0.10	0.21	5.33	98.6	21.2	1.55	2.28
Adrar 003	17	8.5	2.24	13.0	66.8	0.49	0.02	1.28 ± 0.32	2.27	0.49	0.23	0.18	4.88	100.4	20.2	1.60	2.40
Bishunpur	22	7.3	1.97	13.4	69.1	0.39	0.02	1.07 ± 0.20	2.08	0.50	0.24	0.18	4.10	100.4	19.3	1.35	1.96
Y-791558	15	9.2	2.67	13.4	68.0	0.70	0.02	1.38 ± 0.62	1.75	0.50	0.18	0.15	4.30	102.2	21.9	1.68	2.52
Krymka	24	10.4	2.37	13.4	63.7	0.34	0.02	1.37 ± 0.23	2.36	0.47	0.39	0.14	7.09	101.9	18.7	1.90	2.48
GRO 95502	13	7.6	1.38	14.9	71.1	0.57	0.01	1.44 ± 0.18	1.70	0.53	0.48	0.10	2.97	102.8	21.4	1.26	2.35
St Mary's County	3	8.1	1.66	14.7	65.4	0.50	0.13	1.9 ± 1.1	2.65	0.53	0.04	0.08	3.36	99.1	22.1	1.35	3.07
Sharps	3	6.9	1.94	13.4	64.2	0.40	0.03	2.1 ± 1.1	5.70	0.39	0.05	0.18	5.17	100.4	18.0	1.26	3.73
Chainpur	23	7.7	2.95	12.0	67.1	1.20	0.04	1.48 ± 0.36	3.43	0.47	0.27	0.10	3.70	100.5	24.6	1.57	2.99
Tieschitz	none found																

Table 6. Mean compositions of mesostasis in randomly selected chondrules with coexisting olivine compositions of $Fa_{<3}$. One point analyzed per chondrule.

Meteorite	N	Na_2O	MgO	Al_2O_3	SiO_2	P_2O_5	Cl	K_2O	CaO	TiO_2	Cr_2O_3	MnO	FeO	Total	Fa (ol)	Na/Al_{CI}	K/Al_{CI}
Semarkona	21	1.9 ± 1.6	5.12	21.3	53.6	0.01	0.01	0.09 ± 0.08	13.9	0.51	0.34	0.24	1.62	98.8	1.19	0.22	0.11
QUE 97008	9	4.0 ± 2.9	4.29	19.4	56.3	0.01	0.00	0.25 ± 0.27	11.5	0.63	0.41	0.22	1.40	98.4	1.24	0.51	0.32
MET 00526	9	5.6 ± 3.4	4.38	19.9	55.9	0.02	0.00	0.31 ± 0.33	9.12	0.55	0.34	0.30	1.46	97.9	1.27	0.69	0.37
EET 90161	13	3.4 ± 2.1	4.48	23.4	51.9	0.01	0.01	0.08 ± 0.08	13.0	0.57	0.25	0.20	1.81	99.1	1.32	0.36	0.09
NWA 1756	9	6.5 ± 3.9	4.96	21.2	51.8	0.01	0.01	0.40 ± 0.36	8.39	0.62	0.35	0.17	1.64	96.0	1.17	0.75	0.46
MET 96503	11	8.0 ± 2.5	4.22	18.3	54.0	0.01	0.01	0.38 ± 0.19	7.59	0.60	0.41	0.20	3.04	96.8	1.35	1.07	0.51
Adrar 003	4	7.7 ± 6.0	5.22	22.7	53.4	0.00	0.08	0.5 ± 0.5	7.55	0.60	0.21	0.06	2.09	100.1	1.02	0.84	0.50
Bishunpur	11	6.2 ± 2.4	5.18	18.2	56.9	0.01	0.01	0.32 ± 0.15	8.19	0.68	0.67	0.22	1.49	98.0	1.23	0.84	0.42
Y-791558	6	9.3 ± 5.4	2.57	23.2	52.1	0.01	0.02	1.9 ± 1.4	6.61	0.55	0.24	0.03	2.60	99.1	0.91	0.98	1.99
Y-793696	3	11.5 ± 2.4	2.63	18.5	64.9	0.00	0.03	1.1 ± 0.2	1.53	0.75	0.64	0.06	1.31	102.9	1.37	1.52	1.39
Krymka	10	9.2 ± 4.9	3.79	19.9	55.1	0.01	0.02	0.68 ± 0.55	7.00	0.74	0.49	0.10	3.32	100.4	1.23	1.14	0.83
GRO 95502	3	3.8 ± 6.5	10.1	17.8	52.1	0.01	0.00	0.4 ± 0.7	15.8	1.42	0.65	0.02	0.69	102.7	0.75	0.52	0.59
St Mary's County	6	8.0 ± 3.7	3.82	19.6	58.3	0.01	0.16	2.1 ± 1.6	5.20	0.67	0.59	0.05	1.13	99.5	1.96	1.00	2.56
Sharps	6	11.1 ± 4.5	3.04	20.9	59.4	0.05	0.02	0.5 ± 1.1	3.57	0.36	0.22	0.04	2.31	101.6	2.31	1.31	0.63
Chainpur	8	9.8 ± 4.6	2.25	23.1	58.7	0.01	0.07	1.0 ± 0.8	4.26	0.63	0.46	0.03	1.31	101.6	1.07	1.04	1.09
Tieschitz	3	2.6 ± 2.2	18.1	15.9	52.1	0.00	0.02	0.17 ± 0.20	9.35	0.69	0.51	0.15	2.64	102.3	1.05	0.40	0.20

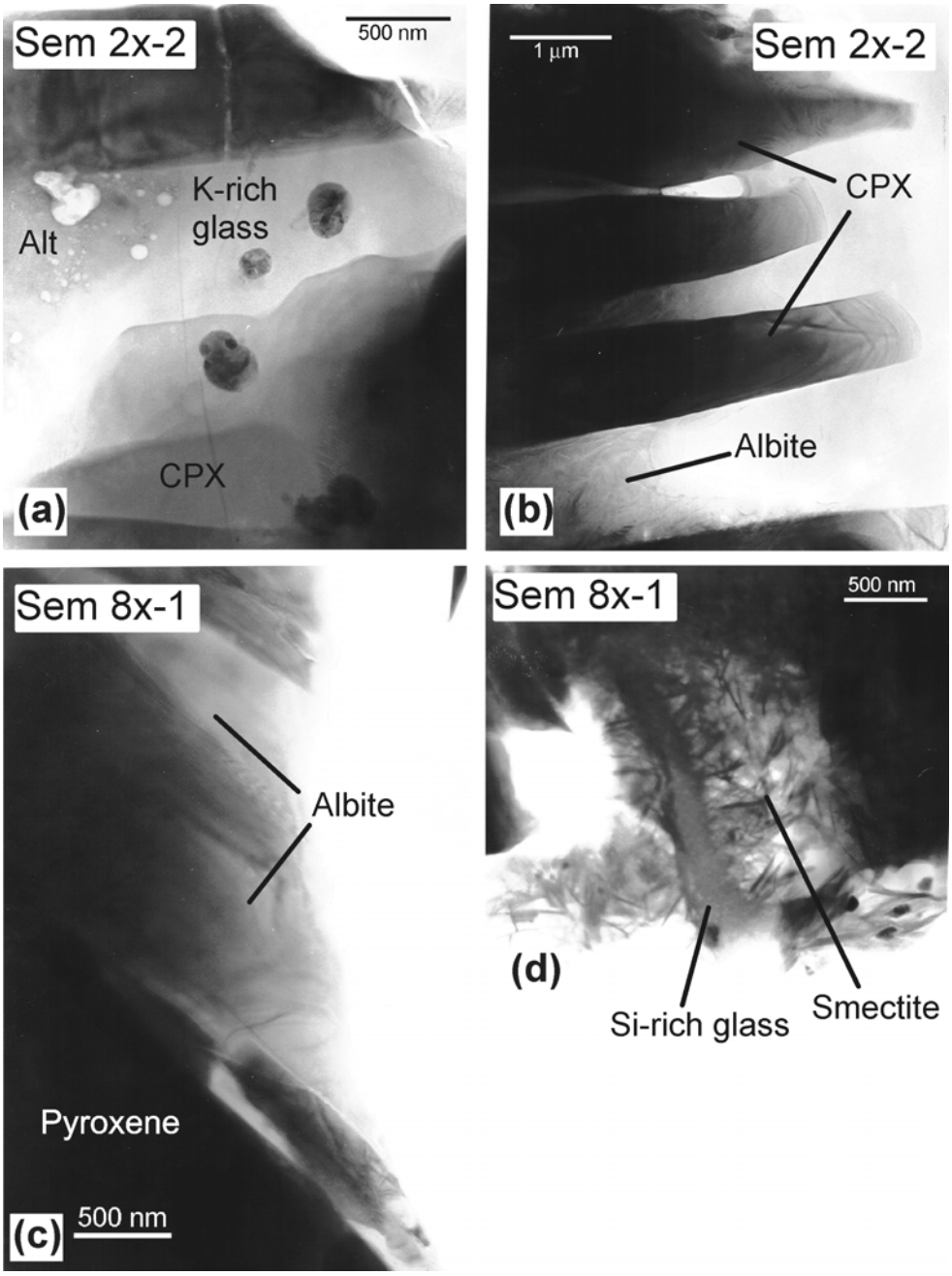

Fig. 7. TEM images of type II chondrules in Semarkona that display a heterogeneous distribution of alkali elements. a) An area of chondrule 2x-2 that appeared to be high in K in X-ray maps. K-rich glass is sandwiched between crystallites of clinopyroxene, showing incipient alteration on the left side of the image. Small iron oxide grains are also present. b) An area of chondrule 2x-2 that appeared to be high in Na in X-ray maps. Crystalline albite occupies the space between clinopyroxene crystallites. c) An area of chondrule 8x-1 that appeared to be high in Na in X-ray maps. Crystalline albite was also found in this chondrule, here shown in contact with coarse-grained low-Ca pyroxene. d) An altered region of chondrule 8x-1, containing Si-rich glassy material and abundant areas rich in smectite.

different sets of chondrules. Again, Semarkona falls at the extreme end of the relationship, with the three other meteorites having high Cr_2O_3 in olivine clustering near it. Krymka has the highest Na/Al in type I chondrule mesostasis of any of the low petrologic type (type <3.3) ordinary chondrites, exceeded only by type 3.4 Sharps.

Composition of Matrix

X-ray maps of several type 3 ordinary and CO chondrites show high levels of sulfur in the opaque matrix compared with other members of the same groups. Figure 10 shows 2 × 2 mm panels taken from larger sulfur X-ray maps of 12

type 3 ordinary chondrites, arranged in the same order as previous plots based of the Cr systematics in olivine. The matrix in Semarkona appears with a pinkish color corresponding to roughly 1.5 wt% S (calibration is done as a simple ratio of pixel counts to the raw number of counts in pixels corresponding to FeS). Queen Alexandra Range (QUE) 97008 shows a few regions that resemble Semarkona, but the matrix is generally lower in S. The next six meteorites, MET 00526, EET 90161, NWA 1756, MET 96503, Adrar 003, and Bishunpur have matrices with apparently lower S than QUE 97008, mostly with greenish colors. In Krymka, GRO 95502, and Chainpur, the matrices appears blue. CO3 chondrites plus Acfer 094 show a similar sequence, as shown in 1 × 1 mm panels of X-ray maps in Fig. 11. Acfer 094 (ungrouped) and ALHA77307 (CO3.0) each appear to have uniformly high S in X-ray maps (>2 wt% on the crude scale), much higher than even Semarkona, and similar to maps for CI and CR chondrites (not shown). Y-81020 appears to have less S in its matrix and resembles the ordinary chondrite QUE 97008 in overall appearance. All of the highest petrologic type CO3 chondrites, ranging from type 3.2 Rainbow and Kainsaz to type 3.8 Isna, appear to have much less S in their matrix than any of the type 3.0s. A map of Colony (also CO3.0) is not shown; most of the matrix in this meteorite is rich in terrestrial weathering products and is low in S.

Quantitative analysis of matrix is a challenging analytical problem due to inhomogeneity on the scale of tens of μm, uncertain corrections, and variable porosity giving low analytical totals. Table 7 shows averages of microprobe analyses for matrix in a wide suite of type 3 ordinary and CO chondrites, including all of those from Figs. 10 and 11. No special corrections were applied to these data. Observations made from X-ray maps were mostly confirmed. Measured FeS contents agree reasonably well with literature data, when available, despite rather different analytical protocols (Table 7). The relationship of the S content of the matrix, normalized to Si, with the Cr_2O_3 content in ferroan olivine in chondrules from the same meteorite is shown in Fig 12a. The ordinary chondrites show a noisy but statistically significant relationship.

Semarkona is clearly different from all of the other meteorites. Of the three other chondrites with high Cr_2O_3 in olivine, two have matrices more S-rich than all meteorites with intermediate or low Cr_2O_3 in olivine. The type 3.3 and higher meteorites all have low S in their matrix (Sharps, Chainpur, St Mary's County, and Tieschitz). Krymka and several other intermediate Cr_2O_3 objects also have low S in their matrix. GRO 95502 seems to have higher S in its matrix than was expected from the X-ray maps and plots above the trend on Fig. 12a defined by other meteorites. The GRO 95502 X-ray map for S was nearly identical to that of Krymka, yet the microprobe analyses were much higher in S. The source of this discrepancy is unknown. Y-793596 and Bishunpur also plot on the high side of the trend in Fig. 12. The thin section of Y-793596 was very small in area and only eight closely spaced analyses were obtained. It is possible that these data are not representative. Bishunpur matrix has an unusual composition not only for S, but also for other elements: Table 7 shows that it is also exceptionally rich in Na, Mg, Al, Si, Cl, K, and Cr and is low in FeO.

The matrix in CO3 chondrites shows a similar distribution of S/Si ratios to that in the ordinary chondrites and quantitative data (Fig. 12b) confirm what was seen in X-ray maps (Fig 5). The meteorites with high Cr_2O_3 content in ferroan olivine can again be divided into two grouplets: Acfer 094 and ALHA77307 with high S/Si, and Y-81020 and Colony with low S/Si, although the extreme degree of weathering in Colony may have affected sulfide grains in the matrix even in the carefully selected regions that were analyzed. Rainbow and Kainsaz plot in a part of the diagram similar to ordinary chondrites such as Krymka.

Sodium in the matrix shows an interesting relationship with the Cr_2O_3 content of ferroan olivine. Among the ordinary chondrites, a plot of Na/Al in the matrix versus Cr_2O_3 in the olivine yields a U-shaped trend (Fig. 13a), broken only by Bishunpur with its anomalous matrix composition. The same two meteorites with high Cr_2O_3 in olivine that have the highest S/Si in matrix also have the highest Na/Al, Semarkona and QUE 97008. The CO chondrites show a hint of a similar trend (Fig. 13b), although none of the meteorites with Cr_2O_3-rich olivine have as high Na/Al in matrix as was found among type 3.0 ordinary chondrites.

Other than the above trends for S (and perhaps for Na), there are no other correlations of elements with Cr_2O_3 in olivine in common to the ordinary and CO chondrite matrix analyses. CaO and MnO in ordinary chondrite matrix both anticorrelate with Cr_2O_3 in ferroan olivine, whereas in the CO group, CaO shows a positive correlation with Cr_2O_3 in olivine and MnO is fairly constant.

Modal Analysis of Components

Results of image-processing studies of X-ray maps in a suite of type 3 ordinary and CO3 chondrites are presented in Table 8. The area analyzed in each chondrite is variable, although larger areas were covered in the coarser-grained ordinary chondrites than in the finer-grained CO3 chondrites. To put these areas in context, a reasonable estimate would be that LL3 chondrites contain ~4 chondrules/mm^2 (or chondrules plus silicate inclusions in CO chondrites), H3 chondrites ~8 chondrules/mm^2, and CO3 chondrites ~40–50 chondrules/mm^2. Thus, the ordinary chondrite images contain cross-sections through 50–100 chondrules, except for ~250 in the case of Semarkona, whereas the smaller-area CO chondrite images show ~100 to >1000 chondrules.

Although the measured volume percentages of matrix, metal, and chondrules were not the target of this study, they are also listed in Table 7. Matrix abundances have been

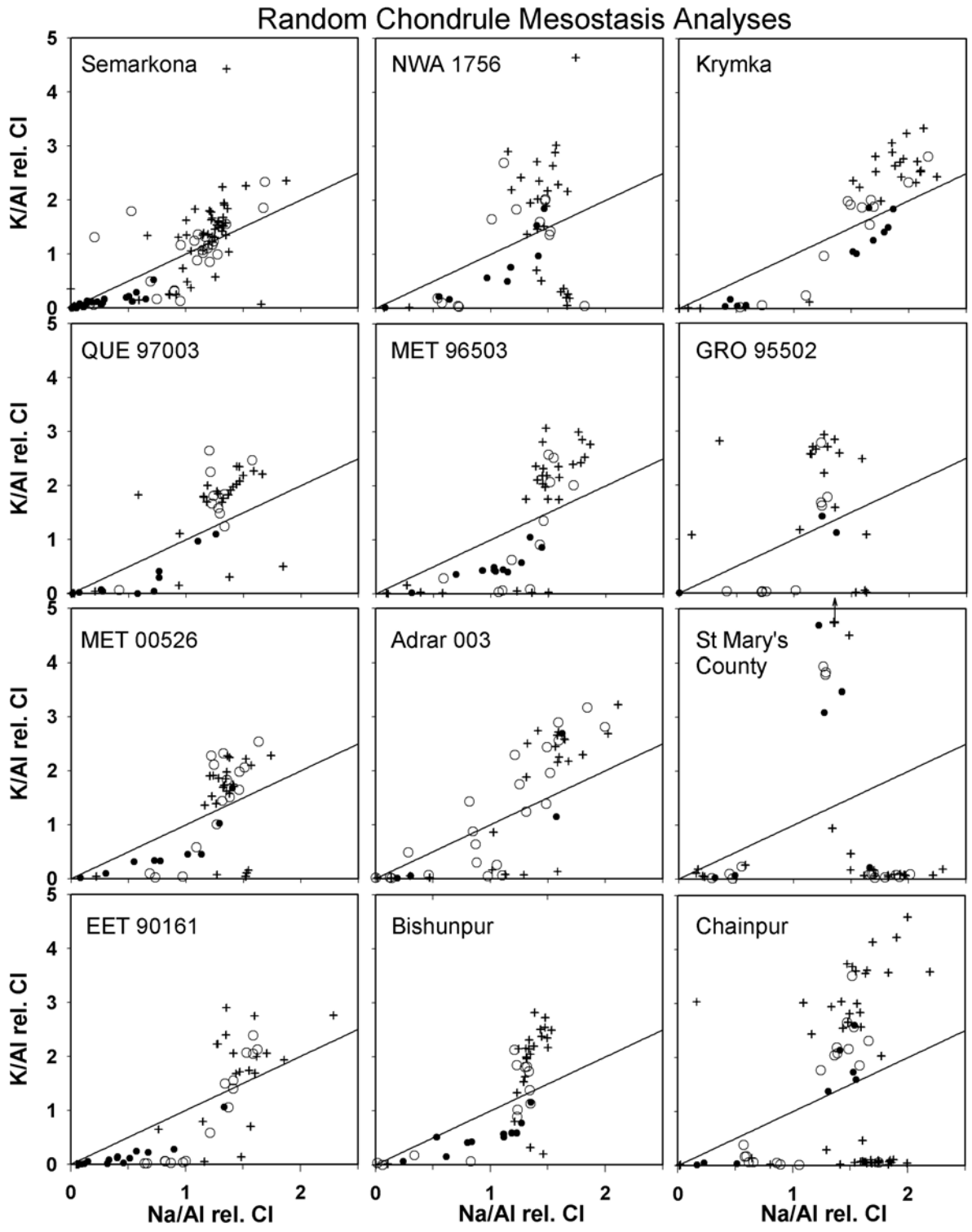

Fig. 8. Compositions of chondrule mesostasis in type 3 ordinary chondrites as determined in surveys of approximately 50 randomly chosen chondrules in each meteorite. Different symbols are used to denote the fayalite contents of coexisting olivine (or ferrosilite content of low-Ca pyroxene, if olivine was absent): closed circles = Fa_0 to Fa_3; open circles = Fa_3 to Fa_{10}; crosses = Fa_{10} and higher. A line showing the K/Na ratio of CI chondrites is shown for reference in each plot. The meteorites are arranged in the same order as in Fig. 4, proceeding from the top left down and to the right.

previously measured by point-counting methods in many of these chondrites; the two methods are quite comparable except for Chainpur and ALHA77307. The measured area of Chainpur was apparently anomalously rich in matrix, the abundance being more than double that found in most type 3 ordinary chondrites. Conversely, the studied area of ALHA77307 was much lower in matrix than was found by Rubin et al. (1985) and closer to those found in other CO chondrites (McSween 1977). Measured metal abundances are highly variable and were clearly affected by weathering in several samples, notably Colony and Rainbow. Modal chondrule abundances appear to be ~10% higher than literature values (cf. Grossman et al. 1988), probably because they were calculated by difference and include the entire population of silicate fragments.

FeS abundances shown in Table 8 were also probably affected by terrestrial weathering in some of the meteorites, especially in Colony and Rainbow. It is possible that other meteorite finds were similarly affected, although clearly not to this extent. Calculated weight percentages of FeS are in reasonably close agreement to literature data, mostly determined by wet chemistry.

The modal amount of FeS in different petrographic locations is strongly related to mean Cr_2O_3 in ferroan olivine in ordinary chondrites. The amount of FeS in chondrule rims is highest in ordinary chondrites with intermediate or high Cr_2O_3 in olivine, with Semarkona having the highest abundance (Fig. 14a). Krymka and GRO 95502 have relatively low abundances of FeS in chondrule rims and resemble the middle type 3 ordinary chondrites Chainpur and St Mary's County. Type 3.8 Dhajala has no discernable FeS in chondrule rims.

The amount of coarse-grained FeS embedded in opaque matrix in ordinary chondrites anticorrelates with Cr_2O_3 in ferroan olivine (Fig. 14b). Again, Semarkona is at one extreme, with the lowest measured FeS in this petrographic location, and the more equilibrated chondrites have the greatest amount of coarse FeS in the matrix. The abundance of FeS in chondrule interiors varies widely (Fig. 14c): the two meteorites with high Cr_2O_3 in olivine are both quite low in chondrule FeS, whereas the chondrites with the most chondrule FeS are types 3.4 Chainpur and 3.8 Dhajala. Chondrites with intermediate Cr_2O_3 in olivine, including 5 low petrologic type samples and two higher-type samples show a wide range of FeS contents inside chondrules.

The abundances of FeS in different locations in CO chondrites are not plotted, partly due to the lack of data for Cr_2O_3 in olivine in the more equilibrated meteorites, and partly due to complications from weathering. Examination of Table 8 shows that two type 3.0 samples, ALHA77307 and Y-81020 have relatively high abundances of FeS in chondrule rims and low abundances of FeS in chondrule interiors and as isolated grains. Colony and Rainbow are low in all FeS components due to weathering. The higher petrologic type

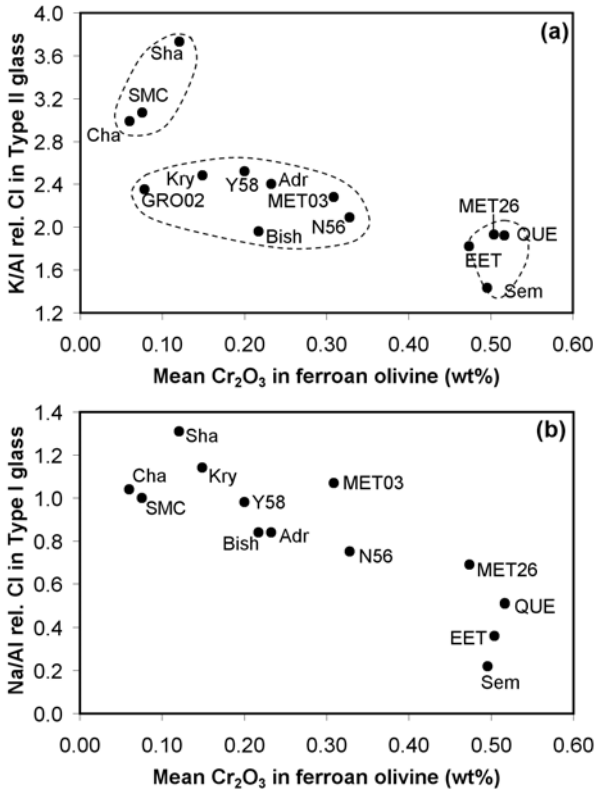

Fig. 9. Compositions of mesostasis in type II chondrules and type I chondrules as a function of the Cr_2O_3 content of ferroan olivine: a) average K/Al ratios for type II chondrules with olivine above Fa_{10}, including only grains that have high alkali contents and that are not dominantly albitic (see text and Table 5). Three grouplets of meteorites are outlined by dotted lines. b) Average Na/Al ratios for type I chondrules with olivine below Fa_3; meteorites with less than four analyses are omitted (see Table 6). All meteorite abbreviations are listed in Table 1.

COs, Kainsaz through Isna, have high abundances of FeS inside chondrules or as coarse matrix grains and, except for Lancé, low abundances of FeS in rims.

DISCUSSION

Petrologic Types of Chondrites

Ordinary Chondrites

The existing decimal scheme for assigning petrologic types to unequilibrated chondrites is based on the convergence of numerous chemical and petrologic parameters that co-vary in a way that is consistent with thermal metamorphism. With increasing metamorphic grade: diffusion homogenizes Fe and Mg in olivine, affecting small matrix grains first; heating results in progressive loss of volatiles and destruction of presolar grains; compositions of metal grains equilibrate; and feldspar increasingly crystallizes during devitrification of glass and recrystallization of matrix (Sears et al. 1980; see also many subsequent papers by the

Table 7. Analyses by electron microprobe of fine-grained matrix in type 3 chondrites (wt%). Samples arranged in order of metamorphic grade as determined in this work.

Meteorite	# Anal	Na_2O	MgO	Al_2O_3	SiO_2	P_2O_5	Cl	K_2O	CaO	TiO_2	Cr_2O_3	MnO	FeO[a]	Ni	FeS[a]	Total	FeS-lit
Ordinary chondrites																	
Semarkona	20	2.16	11.1	2.88	34.2	0.01	0.20	0.37	0.78	0.05	0.24	0.20	27.5	0.62	3.39	80.9	2.4[c]
QUE 97008	15	2.20	12.2	3.39	38.6	0.02	0.03	0.41	0.89	0.06	0.28	0.23	29.8	0.86	2.33	89.4	–
MET 00526	11	1.85	11.2	4.08	40.1	0.00	0.06	0.38	0.85	0.06	0.27	0.23	33.3	0.96	1.18	93.5	–
EET 90161	17	0.78	9.45	2.75	31.0	0.07	0.27	0.19	0.77	0.05	0.24	0.28	43.0	2.11	1.49	91.2	–
NWA 1756	15	0.10	9.73	1.81	31.0	0.06	0.02	0.09	0.75	0.04	0.27	0.34	48.1	0.78	0.65	93.3	–
MET 96503	13	1.22	11.2	4.40	34.5	0.02	0.36	0.40	0.77	0.06	0.24	0.22	33.1	1.66	1.20	88.4	–
Adrar 003	14	0.47	10.9	2.64	35.4	0.14	0.04	0.21	1.84	0.04	0.25	0.45	44.8	0.84	0.39	98.1	–
Bishunpur	13	3.31	14.2	4.93	44.9	0.03	0.33	0.70	1.31	0.09	0.66	0.27	22.9	0.87	2.04	95.0	2.2[c]
Y-791324	15	0.58	11.0	3.30	34.1	0.08	0.11	0.21	0.94	0.05	0.25	0.38	41.3	0.80	0.77	93.2	–
Y-791558	15	0.65	11.8	3.42	34.6	0.10	0.04	0.20	1.10	0.06	0.22	0.35	44.4	1.15	0.59	98.2	–
Y-793596	8	0.14	10.3	1.18	30.2	0.05	0.15	0.02	0.53	0.04	0.26	0.72	48.8	1.12	1.37	94.9	–
Krymka	20	0.82	12.0	3.24	32.7	0.16	0.10	0.17	1.14	0.06	0.25	0.38	43.7	0.98	0.49	95.7	0.49[c]
GRO 95502	14	1.31	10.7	4.02	35.6	0.10	0.21	0.31	1.67	0.08	0.28	0.28	31.6	2.12	1.23	88.4	–
St Mary's County	15	1.31	13.9	3.57	35.5	0.11	0.06	0.33	1.58	0.06	0.26	0.46	37.2	0.42	0.26	94.8	–
Sharps	2	0.46	25.0	1.35	35.0	0.47	0.00	0.04	0.95	0.04	0.46	0.46	36.0	0.30	0.48	100.6	0.82[c]
Chainpur	11	1.31	14.3	3.23	33.2	0.03	0.11	0.18	0.97	0.06	0.30	0.47	31.1	0.50	0.34	85.9	0.77[c]
Tieschitz	15	1.47	17.3	2.72	36.2	0.22	0.13	0.20	1.48	0.08	0.35	0.49	34.3	0.18	0.21	95.1	0.22[c]
CO3 chondrites and Acfer 094																	
Acfer 094[b]	–	0.16	19.1	1.57	33.5	n.d.	n.d.	0.17	2.36	0.08	0.46	0.28	21.7	1.34	5.71	86.4	–
ALHA77307	7	0.46	15.9	3.61	28.0	0.12	0.10	0.17	1.16	0.05	0.31	0.25	27.5	2.45	5.75	81.1	3.9[d]
Y-81020	15	0.15	12.8	2.18	24.0	0.06	0.09	0.24	0.74	0.06	0.26	0.22	38.2	2.06	1.31	81.4	–
Colony	8	0.05	9.22	1.69	22.8	0.18	0.02	0.05	0.62	0.03	0.27	0.20	49.7	1.38	0.50	86.2	–
Rainbow	10	0.02	13.7	3.16	29.9	0.23	0.01	0.03	0.25	0.06	0.37	0.24	43.4	1.68	0.58	93.1	–
Kainsaz	10	0.67	16.9	2.54	30.1	0.17	0.10	0.16	0.74	0.09	0.37	0.42	34.1	0.72	0.41	87.2	0.24[e]
Felix	5	0.39	16.4	3.41	25.6	0.07	0.04	0.04	0.70	0.07	0.30	0.27	29.7	0.37	0.20	77.4	1.2[e]

[a]Calculated after combining sufficient Fe with S to make troilite.

[b]Unpublished analysis by Geiger (Bischoff, personal communication).

References to literature: c) Huss et al. (1981); d) Scott and Jones (1990); e) McSween and Richardson (1977).

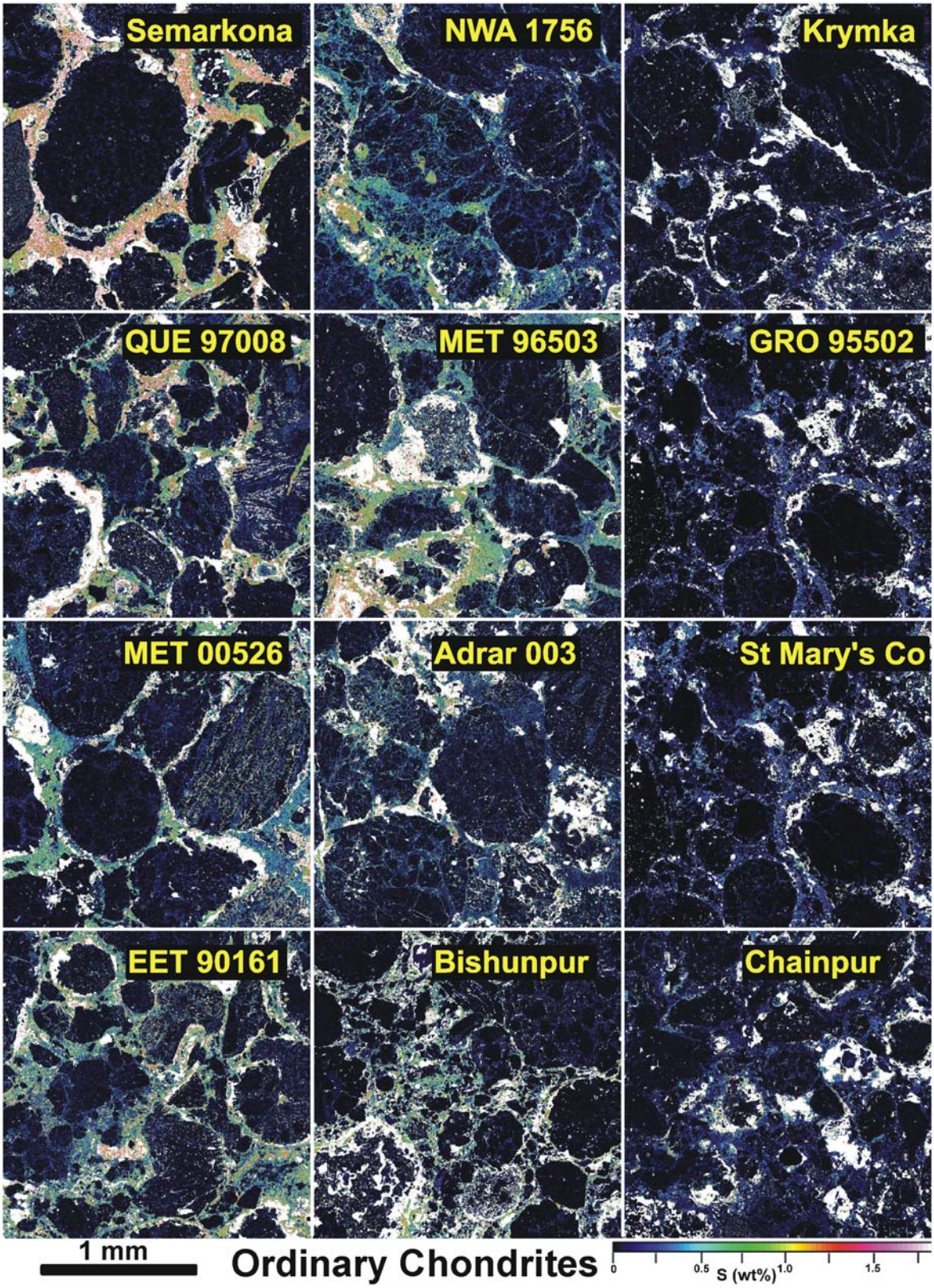

Fig. 10. False color X-ray maps of sulfur in twelve type 3 ordinary chondrites. Images are all 2 × 2 mm and are arranged as in Fig. 8. An approximate sulfur concentration scale is shown at the lower right, crudely calibrated based on the ratio of counts in the pixels to the number of counts in pixels corresponding to pure FeS. Bright white areas are mostly FeS grains. Coarse-grained silicates, including chondrule minerals, appear dark. Blues, greens, and pinks correspond to areas of opaque matrix.

Table 8. Modal analyses of components in unequilibrated chondrites based on image-processing of X-ray maps.

	Area mm^2	Matrix vol%	Lit matrix vol%[a]	Metal vol%	Chdl vol%[b]	FeS isolated vol%	FeS rims vol%	FeS chdls vol%	Metal calc wt%	Matrix calc wt%	Chdls calc wt%	FeS calc wt%[c]	Lit FeS wt%
Ordinary chondrites													
Semarkona	60	16.1	15.6	2.9	76.9	1.0	2.8	0.4	6.98	13.9	73.4	6.2	5.3
EET 90161	14	14.3		1.3	80.2	2.1	1.9	0.3	3.12	12.7	78.3	6.2	
MET 96503	14	9.9		0.7	85.6	1.4	1.7	0.7	1.61	8.8	84.2	5.5	
Adrar 003	14	9.4		3.7	82.8	2.1	1.6	0.4	8.60	8.0	77.8	5.6	
Bishunpur[d]	20	14.4	13.9	5.3	74.2	3.0	2.2	1.0	12.06	11.9	67.9	8.4	6.5
Krymka	22	9.7	12.6	0.6	85.9	2.2	1.4	0.2	1.37	8.7	84.6	5.5	6.0
GRO 95502	14	13.4		1.1	81.8	2.3	1.1	0.4	2.69	11.8	80.1	5.5	
St Mary's County	32	20.5		0.7	74.3	3.1	0.9	0.6	1.69	18.4	73.5	6.5	6.5
Sharps	12	14.0	12.4	2.8	78.7	3.5	0.5	0.4	6.77	12.1	75.1	6.1	5.8
Chainpur	20	29.7	16.1	1.6	63.0	3.4	1.1	1.2	3.80	26.4	61.8	8.2	6.4
Dhajala	5	n.d.	17.2	5.7	71.6	4.2	0.0	1.2	13.1	(14.3)	65.5	7.2	5.1
CO3 chondrites and Acfer 094													
Acfer 094	6	42.0		1.4	51.7	4.7	0.2	0.1	3.6	37.9	51.5	9.2	6.1
ALHA77307	3	25.0	43.1	7.3	65.4	1.7	0.3	0.2	16.7	20.7	59.7	4.4	6.2
Y-81020	2	24.0		3.7	70.3	1.4	0.4	0.3	8.8	20.9	67.5	3.1	4.0
Colony	9	28.8	29	0.0	71.2	0.1	0.0	0.0	0.0	26.8	73.0	0.3	1.5
Rainbow	8	33.4		0.0	65.3	1.1	0.1	0.1	0.0	31.0	67.0	2.1	
Kainsaz	14	24.8	30.0	4.7	67.6	2.3	0.1	0.4	11.0	21.3	63.8	4.1	4.2
Felix	2	32.8	32.9	3.5	60.0	2.9	0.1	0.6	8.4	28.7	57.9	5.2	5.5
Lancé[d]	2	26.9	32.8	1.8	64.5	5.2	0.3	1.3	4.4	23.6	62.5	9.5	6.5
Warrenton	2	n.d.	37.8	4.2	54.6	2.7	0.2	0.4	10.1	(32.9)	52.4	4.7	5.1
Isna	2	42.7	28.7	1.1	53.9	1.4	0.1	0.8	2.8	39.2	54.6	3.5	4.5

[a]Sources of literature data: McSween (1977); Huss et al. (1981); Rubin et al.(1985); Dreibus et al. (1995); Köblitz (2003).

[b]Chondrules, calculated by difference from the modal amounts of matrix, metal, and sulfides; in CO3 chondrites, this also includes CAIs and AOIs.

[c]Calculated by adding FeS based on X-ray map analysis to FeS measured by microprobe in matrix (from Table 2).

[d]A large sulfide-rich nodule was omitted from the modal analysis.

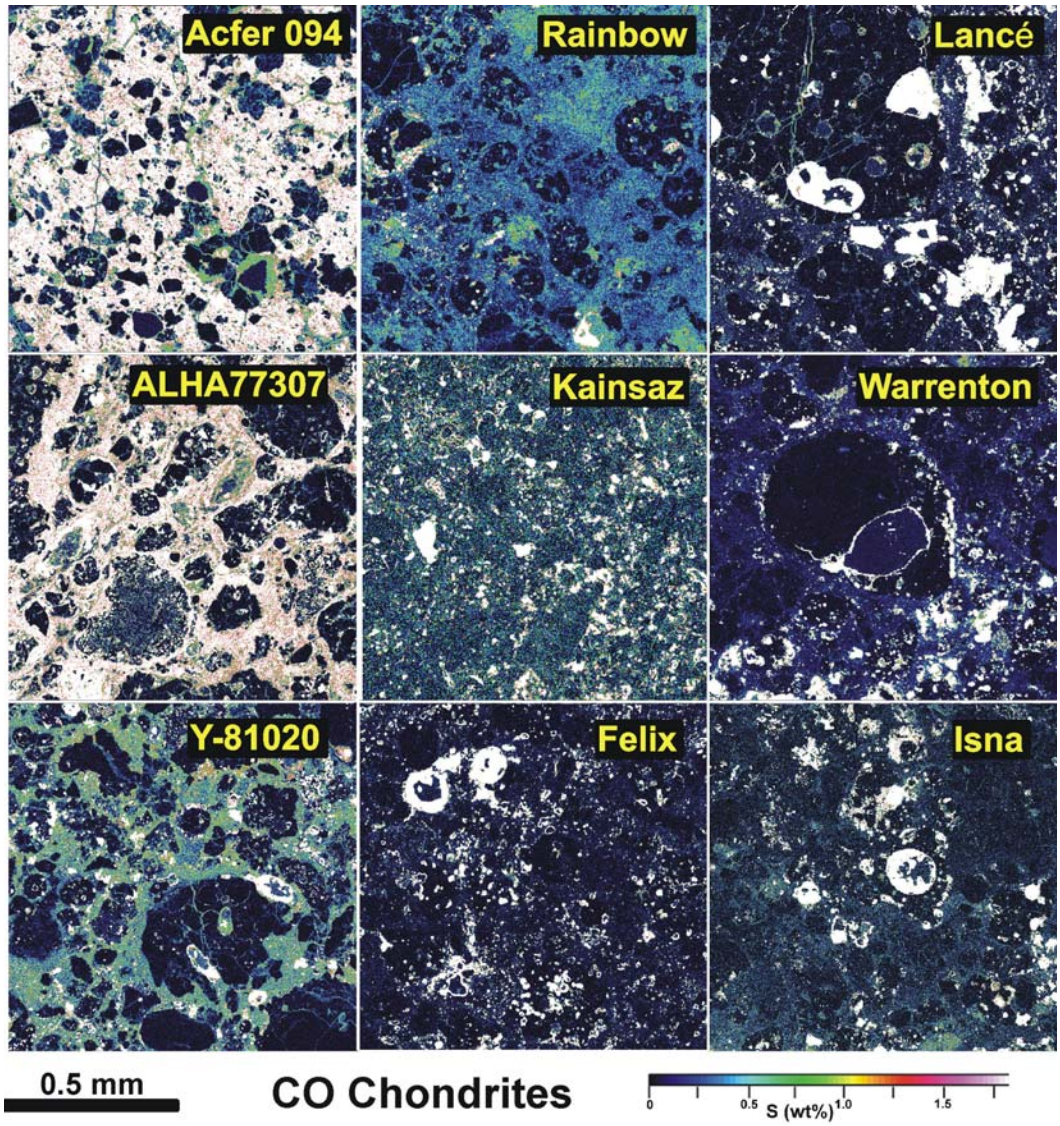

Fig. 11. False color X-ray maps of sulfur in Acfer 094 plus 8 CO3 chondrites. All images are 1 × 1 mm, arranged in order of petrologic type. See Fig. 9 for explanation of colors. In Acfer 094 and ALHA77307, the matrix appears pinkish white and is barely distinguishable from grains of FeS that appear white.

Sears group reviewed by Huss et al. 2005). Because TL sensitivity, a measure of the degree of crystallinity of feldspar, varies by several orders of magnitude across the type 3 chondrites, it has traditionally been used as the strongest indicator of low petrologic type. As discussed above, at the lowest petrologic types the TL system cannot accurately discriminate between various levels of metamorphism, and therefore other indicators are used to make the distinctions. This can readily be seen in an examination of the first two columns of Table 9: the correlation coefficient between measured TL sensitivity and the literature recommended petrologic type for the meteorites below petrologic type 3.2 included in the present study is near zero.

The data in the present study provide a way to extend the quantitative Sears scheme, enabling the assignment of accurate petrologic types to highly unequilibrated chondrites as well. They provide at least five new parameters that show strong co-variation at the lowest end of the metamorphic sequence: Cr_2O_3 content of ferroan olivine, K/Al ratio of glass in type II chondrules, Na/Al ratio of glass in type I chondrules, S and Na content of the matrix, and the modal abundances of sulfides in various petrographic locations. These are very much analogous to the set of parameters outlined in the original study that subdivided type 3 ordinary chondrites (Sears et al. 1980) in that one has the sensitivity and range to form the backbone of a classification scheme while the others can be used to support classification decisions.

Compared to most other classification parameters, both in the literature and developed in this paper, the measurement of Cr_2O_3 in ferroan olivine is one of the most straightforward to make and is nearly unaffected by processes such as aqueous alteration and terrestrial weathering. Even highly weathered

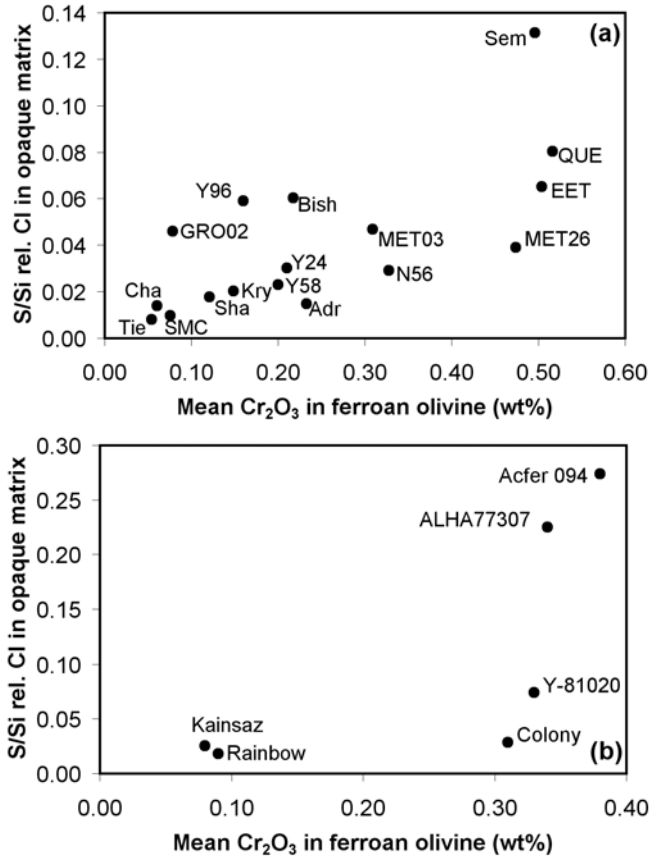

Fig. 12. Plots showing the relationship between the mean S/Si content of opaque matrix to the mean Cr_2O_3 content of ferroan olivine in a) ordinary chondrites and b) CO chondrites plus Acfer 094. Matrix data are from Table 7. Meteorite abbreviations are listed in Table 1.

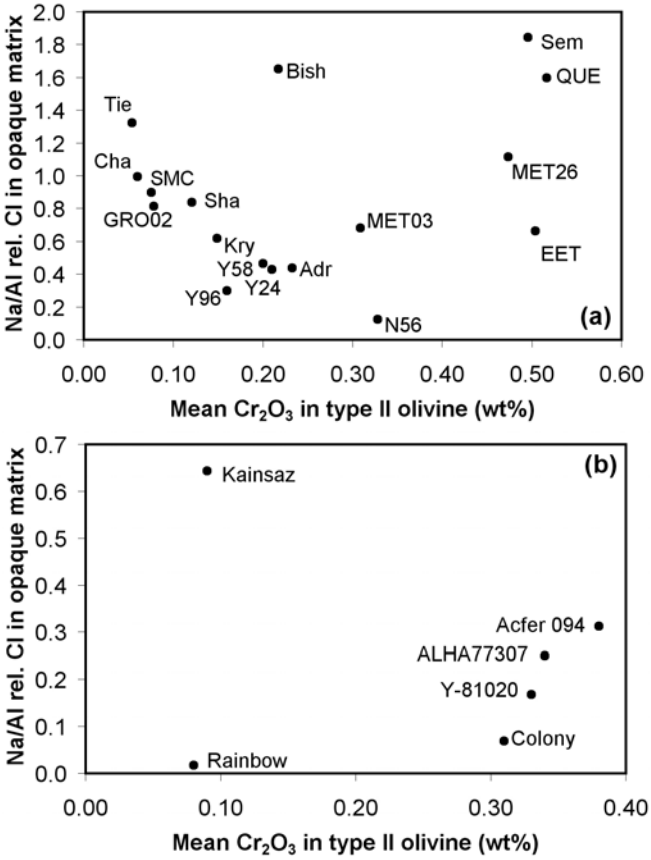

Fig. 13. Plots showing the relationship between the mean Na/Al content of opaque matrix to the mean Cr_2O_3 content of ferroan olivine in a) ordinary chondrites and b) CO chondrites plus Acfer 094. Matrix data are from Table 7. Meteorite abbreviations are listed in Table 1. Bishunpur breaks the U-shaped relationship for the ordinary chondrites in (a), and has anomalous concentrations of other elements as well (see text).

meteorites such as Roosevelt County (RC) 075 and Colony preserve abundant fresh olivine. Surveys of Cr_2O_3 in ferroan olivine are essentially no different than those made for FeO in olivine, which have long been used to classify chondrites. The Cr_2O_3 content of olivine varies from ~0.5 wt% in the type 3.0s down to ~0.05 wt% in the middle of the type 3 ordinary chondrite sequence, a range of about one order of magnitude, with most of this drop occurring by type 3.2. CO3 chondrites show a somewhat smaller range of Cr_2O_3 in olivine, but again the variation occurs mostly between types 3.0 and 3.2. However, this parameter is even more sensitive than is indicated by its range. As could be visualized in the histograms of Figs. 4 and 5, not only does the mean Cr_2O_3 content of ferroan olivine change, but the degree of scatter in the data does also. A plot of the standard deviation versus the mean of Cr_2O_3 in olivine in ordinary chondrites (Fig. 15a) shows how the peak initially broadens with little change in mean, then the mean shifts to lower values and the peak progressively narrows.

We propose to subdivide the type 3 ordinary chondrites further and more accurately on the basis of Fig. 15a and we show the results in Table 9. Semarkona, with its narrow Cr_2O_3 distribution in ferroan olivine and high mean, is designated to be type 3.00, adding a second decimal place to the existing classification. The next three meteorites, QUE 97008, MET 00526, and EET 90161, in which the Cr_2O_3 distribution broadens but the mean does not change, are designated type 3.05. In support of the distinction between Semarkona and the three 3.05 chondrites is the high value displayed by Semarkona for S in matrix, plus its extreme values for K/Al in type II glass, Na/Al in type I glass, and the abundance of FeS in chondrules and rims.

Type 3.1 is assigned to those meteorites in which the mean Cr_2O_3 has fallen significantly below that shown by type 3.0 but which still contain a population of olivine in the type 3.0 range as seen in Fig. 4. In Fig. 15a, the type 3.1s occupy the center of the diagram and are arbitrarily subdivided into type 3.10 for those meteorites nearest to type 3.0 in Cr_2O_3 content and type 3.15 for those in which the mean has fallen to below about half of type 3.0 values and that show a significant decrease in the standard deviation.

The issue of how to assign meteorites like Krymka and

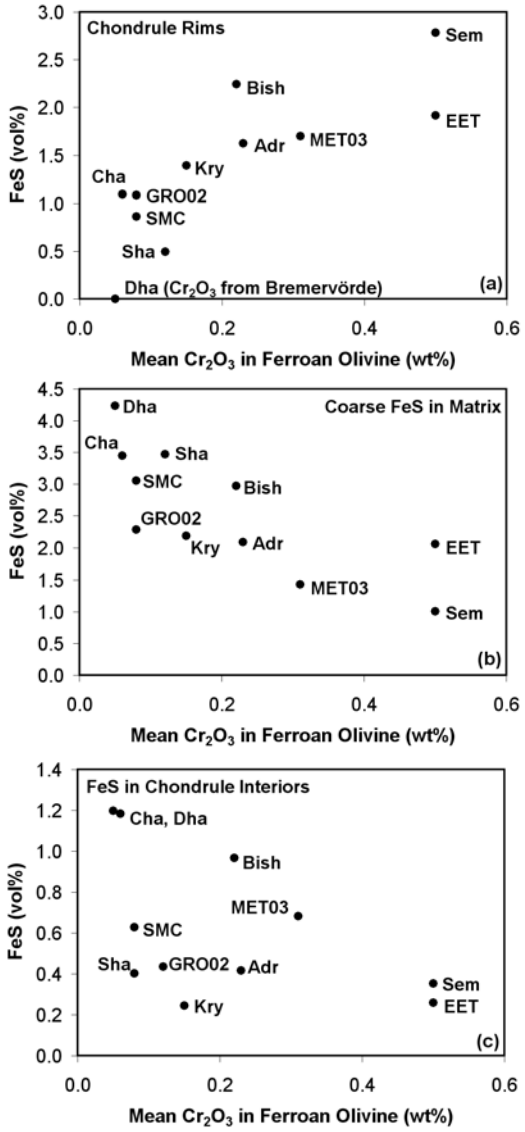

Fig. 14. Abundances of FeS in a) chondrule rims, b) coarse matrix grains, and c) chondrule interiors in ordinary chondrites, plotted as a function of mean Cr_2O_3 content of ferroan olivine. Olivine in Dhajala (H3.8) was not measured, so the value for Bremervörde (H/L3.7) was substituted. Sulfide data are from Table 8. Meteorite abbreviations are listed in Table 1.

GRO 95502/95544, which have low mean Cr_2O_3 and narrow histograms, is more difficult. Krymka has traditionally been classified as a type 3.1 ordinary chondrite, primarily on the basis of induced TL. However, the volatile element content of Krymka is quite low, comparable with middle type 3 ordinary chondrites (Anders and Zadnik 1985). Many of the studies that have been helpful in distinguishing type 3.0 from 3.1 chondrites (e.g., DeHart et al. 1992; Sears et al. 1990) have not included any type 3.2 chondrites for comparison, mainly because few of them are known. On the basis of the low TL sensitivity of these meteorites, but also the low Cr_2O_3 in olivine and other properties indicating mild metamorphism (see below), Krymka and GRO 95502/95544 are placed in the type 3.2 category.

Note that these refinements to the definitions of types 3.0, 3.1, and 3.2 are conservative and do not conflict with literature assignments of petrologic types that were based on a combination of low TL sensitivity (and glow curve shape) and observations of CL properties of chondrules and mesostasis compositions. The only reassignments by 0.1 units are those discussed above for Krymka (3.1 to 3.2), moving the poorly characterized meteorite Y-793596 from 3.0 to 3.2, and changing the virtually uncharacterized meteorite MET 00536 from 3.2 to 3.05.

The new petrologic type assignments proposed for ordinary chondrites in Table 9 are supported by data for presolar grain abundances. Huss and Lewis (1994, 1995) determined the properties of presolar diamond and SiC in Semarkona, Bishunpur, and Krymka; Huss et al. (1998) examined RC 075; and Huss (personal communication) has analyzed Adrar 003. Semarkona is clearly the most primitive of all five meteorites, with high abundances of diamond and SiC plus a strong low-temperature release of Xe-P3, similar to that in Orgueil. Bishunpur, RC 075 and Adrar 003, which are here classified as types 3.15, 3.10, and 3.10, respectively, have noble gas release curves and diamond abundances that are similar to each other and consistent with a higher degree of thermal processing than experienced by Semarkona. The presolar diamond abundance of Krymka (for which there is no Xe-P3 measurement) is similar to that in Bishunpur, but the abundance of SiC is significantly lower than in Semarkona, Bishunpur, or Adrar 003, suggesting that Krymka is the most metamorphosed of the five meteorites, consistent with the new classification of type 3.2.

The issue of how brecciated chondrites behave in the olivine Cr system can be addressed by examining data for Ngawi, a mixture of types 3.1 and 3.6–3.7 material. This meteorite falls off the ordinary chondrite trend at higher standard deviation or lower mean Cr_2O_3 than other samples. Its anomalous position can be precisely modeled as a mixture of ~22% chondrules like those in Semarkona plus 78% chondrules like those in Bremervörde, which would produce Cr_2O_3 coordinates of mean = 0.15 and σ = 0.20, identical to the measured values (Table 2), and would duplicate the Ngawi histogram in Table 4. None of the other meteorites in this study have been described as mixtures of different petrologic type components like Ngawi, although it is possible that some poorly described meteorites could be like this. Thorough classification of any meteorite would certainly require examination for this type of brecciation before interpretations are made from a diagram such as Fig. 15a.

CO Chondrites

The CO3 chondrites show a similar relationship to the ordinary chondrites on a standard deviation versus mean Cr_2O_3 in olivine plot (Fig. 15b), shifted to lower Cr_2O_3

Table 9. Suggested petrologic types for ordinary chondrites and underlying TL sensitivity data.

		Petrographic type	
Name	TL sensitivity × 1000[a]	Literature[a]	This work[b]
Semarkona	4.5 ± 2.0	3.0	3.00
QUE 97008	3 ± 1	3.0	3.05
MET 00526	–	3.2	3.05
EET 90161	4 ± 1	3.0	3.05
NWA 1756	–	3.0/3.2	3.10
NWA 3127	–	n.d.	3.10
RC 075	22 ± 4	3.1	3.10
MET 96503	6 ± 2.0	3.1/3.2	3.10
Adrar 003	4.6 ± 0.13[c]	3.1	3.10
Bishunpur	5 ± 3	3.1	3.15
Y-791324	4.8 ± 2.5	3.0/3.1	3.15
Y-791558	6.5 ± 0.6	3.1	3.15
Y-793596	2.5 ± 0.6	3.0	3.2
Krymka	3.0 ± 0.2	3.1	3.2
GRO 95502	1 ± 1	3.1/3.2	3.2
GRO 95544	3 ± 1	3.1/3.2	3.2
St Mary's County	34 ± 8	3.3	(3.3)
Sharps	80 ± 30	3.4	(3.4)
Chainpur	70 ± 10	3.4	(3.4)
Tieschitz	200 ± 70	3.6	(3.6)
Bremervörde	600 ± 200	3.7	(3.7)
Dhajala	≡1000	3.8	(3.8)
Ngawi	250 ± 130	3.1–3.7	3.0(–3.7)

[a]See Table 1 for references to petrologic types and TL data.
[b]Numbers in parentheses were not subject to revision based on data presented in this paper.
[c]A second sample gave the result of 11 ± 5.

values. The three type 3.0 CO chondrites all plot with similar mean Cr_2O_3 but with variable standard deviations. If an analogy could be drawn to the ordinary chondrites, ALHA77307 might be designated type 3.00 and Colony and Y-81020 might be type 3.05. However, with no type 3.1 CO chondrites for comparison, it is not possible to examine a broad range of petrologic types and such division is not recommended at this time, though ALHA77307 does appear to be the most primitive. In addition to its position on Fig. 15b, ALHA77307 has by far the highest matrix S content of any CO chondrite, reinforcing the notion that it is less metamorphosed than meteorites such as Y-81020. This is also supported by presolar grain data (Huss et al. 2003), showing that ALHA77307 is more primitive than Colony. The ungrouped relative of CO chondrites, Acfer 094, falls in the same range as the CO3.0 trio on Fig. 15b and is also clearly a type 3.0 chondrite. Rainbow and Kainsaz plot in a position consistent with their classification as CO3.2 by analogy with the ordinary chondrites Krymka and GRO 95502.

CV and Other Chondrite Groups

The proposed subdivision of CV3 chondrites into a metamorphic sequence by Guimon et al. (1995) is not widely used and conflicts with recent work by Bonal et al. (2004). The data for Cr_2O_3 in olivine available so far do not resolve this issue, although additional measurements may yet do so. The most complete CV data set in Fig. 5 and Table 2 is for Vigarano, which was classified by Guimon et al. (1995) as type 3.3. The olivine data are virtually identical to those of the type 3.2 CO chondrites Kainsaz and Rainbow. Without any olivine data from a CO3.3 chondrite for comparison or a complete range of CV data, there is no basis for trying to revise the literature classification of Vigarano. Kaba was classified by Guimon et al. (1995) as type 3.0 and by Bonal et al. (2004) as 3.1. Data in Fig. 5 for Kaba olivine show a broad distribution, with a number of analyses in the low Cr_2O_3 range of Vigarano. These data are much more consistent with the type 3.1 designation than type 3.0 by analogy with ordinary and CO chondrite distributions. The present data for Leoville olivine are very sparse, but indicate that this chondrite is at most a type 3.1, possibly consistent with the Guimon et al. (1995) classification of 3.0, and probably not consistent with the Bonal et al. (2004) assignment of type 3.1–3.4. The three Allende olivine analyses all have very low Cr_2O_3, provisionally indicating type 3.2 or higher.

Other chondrite groups contain ferroan olivine that could be analyzed in future studies, including CI, CM, CR, CK, R, and Kakangari-like meteorites. Literature data for Cr_2O_3 in ferroan olivine from CR and CM chondrites are consistent with most of them being unmetamorphosed (e.g., Ichikawa and Ikeda 1995; Brearley and Jones 1998), though there are thermally metamorphosed CM chondrites that could be examined.

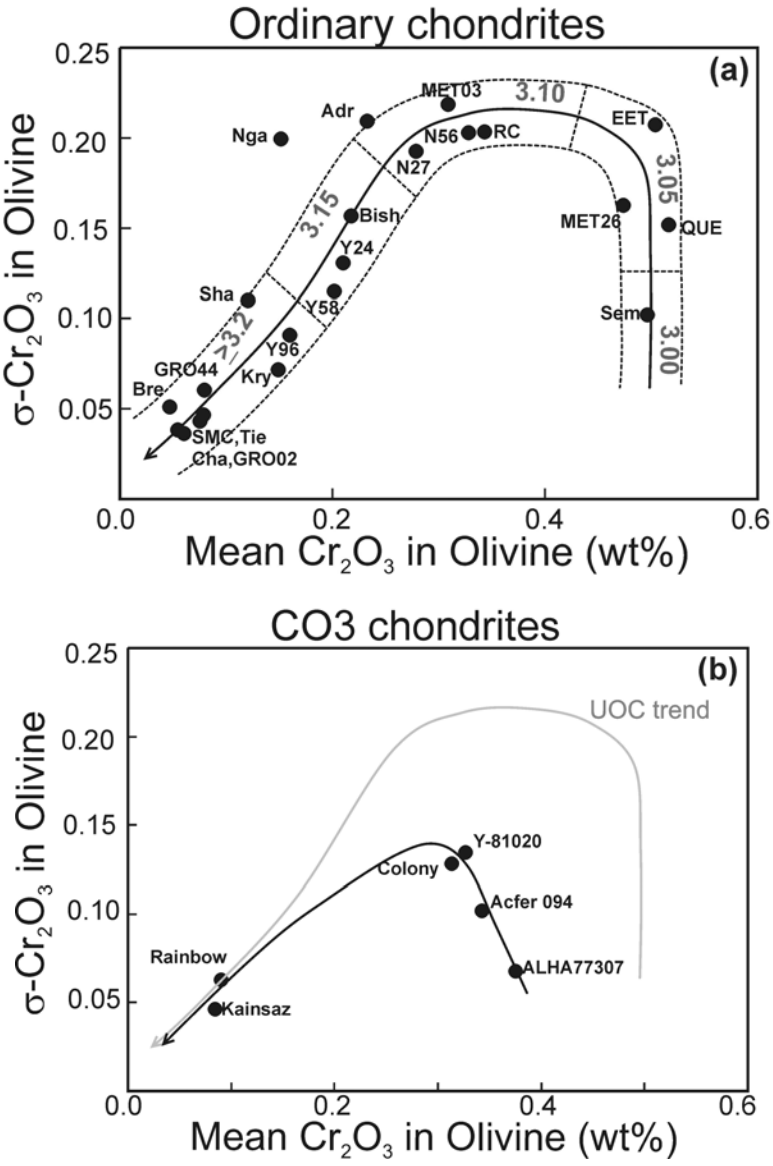

Fig. 15. Plots of the standard deviation versus the mean of the Cr_2O_3 content of ferroan olivine: a) in ordinary chondrites and b) in CO chondrites plus Acfer 094. The solid line in a) is a hand-drawn trend through the data, with parallel dotted lines denoting the approximate spread of points. Suggested divisions for subdividing the type 3.0 and 3.1 chondrites are shown. Type 3.2 and higher petrologic types cannot be easily distinguished. Ngawi, a breccia of type 3.1 and 3.6/3.7 material, plots above the trend defined by the other meteorites (see text). The CO chondrites in (b) show a different trend (black line) than do ordinary chondrites (gray reference line). Meteorite abbreviations are listed in Table 1.

Metamorphic Processes

Exsolution Features in Olivine

Dodd (1973) discovered that olivines in unequilibrated chondrites like Sharps had much higher Cr_2O_3 contents than those in types 4–6 chondrites and attributed the difference to the formation of chromite during progressive metamorphism. The point in the metamorphic sequence at which Cr_2O_3 in olivine begins to change was pushed back to between types 3.0 and 3.3 by McCoy et al. (1991) and then to between types 3.0 and 3.1 by DeHart et al. (1992), although the latter was based on Krymka, which is classified as type 3.2 in the present work for this very reason. Ashworth (1979) found olivine grains in equilibrated H chondrites that contained exsolved chromite, some of which were very fine-grained and appeared to be the product of homogeneous nucleation during metamorphism, and others that were coarser and nucleated on grain boundaries. He also noted that evidence for these phenomena in type 3 chondrites had not yet been found. Microprobe studies by Johnson and Prinz (1991) and experimental work by Jones and Lofgren (1993) showed how chromite and olivine react and equilibrate during metamorphism and annealing in low petrologic-type ordinary chondrites.

The present data greatly expand what is known about the

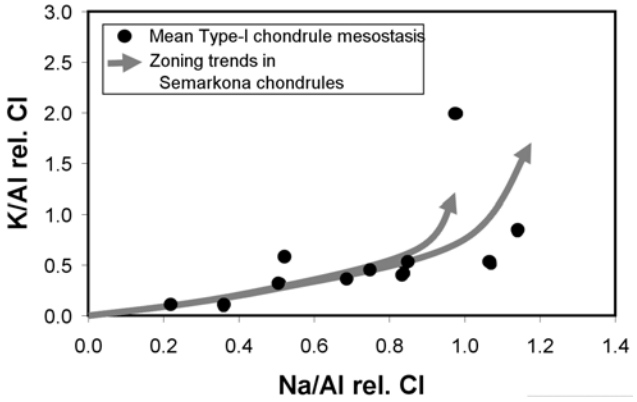

Fig 16. Comparison of the alkali element trends in zoned type I chondrules in Semarkona (arrows, after Grossman et al. 2002) with mean type I chondrule mesostasis composition in types 3.0–3.2 chondrites (Tables 1 and 6). On a plot of K/Al versus Na/Al, the zoning trends follow the same path as the metamorphic trend defined by the chondrites and are probably due to the same process.

phenomenon of Cr exsolution from olivine but are not adequate to account completely for the reactions involved. The progression from clear, igneously zoned olivine grains in type 3.0 to grains crowded with aligned Cr-rich inclusions in their cores, clear outer zones, and Cr-rich surface coatings in type 3.1 to grains with scattered large chromite grains in their cores and chromite rims in higher petrologic types are consistent with the TEM observations made by Ashworth (1979). In the cores of olivines in type 3.1 chondrites, abundant homogeneous nucleation of a Cr-rich phase occurs, producing fine, needle-like precipitates aligned along preferred crystallographic directions in the olivine. Nucleation also occurs freely along the grain boundaries between olivine and adjacent phases, resulting in precipitation of a band of the Cr-rich phase in that location and a depleted zone in the olivine just below the surface where bulk diffusion has transported Cr out of the olivine grain. Apparently, continued heating to form higher-petrologic-type chondrites resulted in the coarsening of Cr-rich precipitates in olivine cores, presumably to minimize their surface energy, to the point where they formed much larger, equant grains (identifiable as chromite) that are visible in the microprobe and can be avoided during olivine analysis. However, clearly some of the fine precipitates survive intact all the way to petrologic types 4–6, as observed by Ashworth (1979).

The question of what chemical reaction drives the exsolution remains an open one. First of all, it is still not actually known whether the fine Cr-rich precipitates observed here and by Ashworth (1979) are chromite. Ashworth was able to determine that some of the coarser precipitates along grain boundaries were chromite, but could not analyze the homogeneously nucleated particles. Second, the valence state and site occupancy of Cr in chondritic olivine are not well known. One direct measurement has been reported in an abstract: Sutton et al. (1996), using microXANES, reported that about 50% of the Cr in type II Semarkona chondrules was present as Cr^{2+} and 50% as Cr^{3+}; in the CO3.0 ALHA77307, they found that about 25% of the Cr was divalent. Dodd (1973) looked for chemical evidence for various substitutions by which Cr^{3+} could be present in olivine and was largely unsuccessful. The present body of analyses on olivine in type 3.0 chondrites also does not contain evidence to support, for example, substitutions such as

$$Cr^{3+}_{VI}Al^{3+}_{VI} \Leftrightarrow (Fe, Mg)^{2+}_{VI}Si^{4+}_{VI} \quad (1)$$

or

$$Cr^{2+}_{VI} \Leftrightarrow (Fe, Mg)^{2+}_{VI} \quad (2)$$

Third, it is not clear that all of the products of exsolution are known. Neither Ashworth (1979) nor the present work have identified any precipitates observed in olivine other than the fine crystallites assumed to be chromite. However, Ashworth did not study highly unequilibrated chondrites and the present study does not include TEM work on olivine. In short, the exact mechanisms and phases involved in the exsolution of the Cr-rich precipitates are not fully characterized.

If it is correct that the exsolved phase in olivine from type 3.1 chondrites is chromite and that there are no products of the reaction other than chromite, it is difficult to write a chemical reaction for this process. The logic used by Ashworth (1979) seems to present the only solution. If Cr were present in the octahedral sites of olivine as Cr^{2+}, one could write an oxidation reaction to produce chromite. If Fe^{2+} had served as the oxidizing agent, then metallic Fe and an SiO_2-rich phase, probably pyroxene, would be among the reaction products along with chromite. If Cr were present as Cr^{3+} in the octahedral sites, charge balanced by tetrahedral Al or a monovalent ion such as Na (there is no evidence for either of these), then direct exsolution of chromite would still produce a SiO_2-rich phase and a symplectic texture. Ashworth's solution was to suggest that chondritic olivine initially contained Cr^{3+} in both tetrahedral and octahedral sites, with the substitution

$$Cr^{3+}_{VI}Cr^{3+}_{IV} \Leftrightarrow (Fe, Mg)^{2+}_{VI}Si^{4+}_{IV} \quad (3)$$

This unusual substitution could be the product of rapid cooling in chondrules. Exsolution of chromite from such an olivine would form no reaction products other than chromite and a Cr-depleted olivine.

Every ferroan olivine grain in the type 3.0 chondrites studied here, including Semarkona, ALHA77307, Acfer 094, and many CR and CM chondrites for which there are literature data, has high Cr contents. In the ordinary and CO chondrites, and probably the CVs as well, metamorphism always produces the same effects, indicating that the oxidation state and site occupancy of Cr in olivine was probably similar prior to metamorphism. If quenching from

high temperatures is necessary to produce olivine with tetrahedral Cr^{3+}, then all of the ferroan olivine in these chondrites, including isolated grains, formed in chondrules and cooled at a rate that was high enough to preserve this state prior to accretion.

Crystallization of Albite from Chondrule Mesostasis

The heterogeneous distribution of alkalis in chondrule mesostasis in ordinary chondrites, when present, is due to the occurrence of two coexisting phases, K-rich glass and nearly K-free albitic feldspar. The overall abundance of albite in these chondrules and the fraction of chondrules containing albite increase with petrologic type, strongly indicating that albite crystallization is a metamorphic effect.

In chondrules with coexisting K-rich glass and albite, inclusions and embayments in olivine and narrow gaps between phenocrysts almost always contain the glass, whereas broad areas of mesostasis contain either albite, glass, or both. The protection of glass in inclusions and other narrow spaces in chondrules suggests that some kind of metasomatic process is at work, perhaps involving transport of material (or heat) into chondrules from their surroundings. In some of these objects, albite occurs preferentially around the periphery, consistent with the idea that the chondrule was interacting with the environment. However, other chondrules contain albite in the core and glass near the surface, which conflicts with this interpretation. A better explanation for these phenomena may be that crystallization of albite was controlled by available nucleation sites. Glassy inclusions, embayments, and narrow areas between phenocrysts tend to be poor in accessory minerals and are almost entirely surrounded by large olivine grains, whereas the open areas of mesostasis are rich in clinopyroxene and other crystallites (e.g., phosphates, sulfides, chromite, and Fe oxides) and may be adjacent to surfaces of large orthopyroxene grains as well as olivine. These differences may be enough to cause albite to nucleate in the broader areas, although it is unclear which phase may be enabling nucleation.

The composition of glass coexisting with albite, especially the K/Al ratio, is also a function of petrologic type. Essentially, the more metamorphic albite that has crystallized, the more fractionated the residual glass becomes. Using the composition of glass in type II chondrules in Semarkona from Table 5 and any of the albites ("Na-rich mesostasis") from Table 4 (glass analyses in Table 4 probably have Na too low), it is possible to model this process. Progressive crystallization of ~40% of this albitic component would raise the K/Al ratio of residual glass from 1.4 CI to over 2.5 CI without greatly changing major elements such as Al_2O_3 and SiO_2.

Open System Behavior of Alkalis in Chondrules During Metamorphism

Although average type II chondrule glass compositions evolve in a way that is consistent with progressive devitrification of mesostasis to form albite, individual chondrules did not behave as closed systems during metamorphism. There is no relationship between the composition of glass and the amount of albite that has crystallized in single chondrules, as is evident in both Semarkona and Chainpur chondrules in Tables 3 and 4. For example, Semarkona chondrules 7-4, 2x-2, and 8x-1 contain glass with nearly identical K/Al (Tables 3 and 4), despite the fact that mesostasis is nearly completely crystalline in the first two, but not in the third. As a result, chondrules 7-4 and 2x-2 almost certainly have highly fractionated bulk K/Na. Chainpur chondrules that are rich in alkalis and are presumably mostly type II (Grossman and Wasson 1982; Kurat et al. 1984), show wide variations of bulk K/Na, ranging on Fig. 8 from near the cluster of mesostasis points with high K/Na to near the x-axis where albitic mesostasis plots. If the chondrules behaved as closed systems during metamorphism, then bulk chondrule compositions would not change as albite crystallized. All of this indicates that components were being exchanged between type II chondrules or between these chondrules and matrix during all stages of metamorphism.

Previous workers have shown that type I chondrules also behaved as open systems during parent body processing in primitive ordinary chondrites. The mesostasis in exterior portions of many type I chondrules in Semarkona is rich in alkalis and water; such mesostasis zoning is the result of metasomatism during aqueous alteration on the parent asteroid (Grossman et al. 2002; Grossman and Alexander 2004). This aqueous alteration probably occurred during the incipient metamorphism that caused albite crystallization in some type II chondrules in Semarkona, with the entire process better characterized as "fluid-assisted metamorphism."

The coincidence of aqueous and metamorphic processes can be demonstrated by comparing the metamorphic trends across all the low-type 3 ordinary chondrites with the zoning trends preserved just in Semarkona chondrules. Figure 8, Fig. 9b, and Table 6 show that Na enters type I chondrules during metamorphism, raising the Na_2O content of mesostasis, a feature that is also well documented in the literature (McCoy et al. 1991; Hewins 1991; Sears et al. 1995a; Alexander et al. 2000). This process apparently occurred without devitrification of the glass: chondrites like Chainpur contain many type I chondrules with clear, isotropic glass that is rich in alkalis, which is a metamorphic overprint. Figure 16 shows that the zoning trends in Semarkona chondrules, which have been attributed to aqueous processes, are identical to the metamorphic trend shown by the mesostasis in the suite of ordinary chondrites of type 3.2. This is undoubtedly because the two trends are manifestations of the same phenomenon. In Semarkona, the process has simply not proceeded far enough to cause homogenization of mesostasis in type I chondrules, resulting in zoned chondrules.

Mobility of Sulfides

The decrease in S content of opaque matrix, decrease in the abundance of FeS in chondrule rims, and increases in abundance of FeS in coarse matrix grains and chondrule interiors are probably all part of the same metamorphic process, one that involves the progressive coarsening of sulfide grains throughout the meteorite.

Extremely fine-grained sulfides were noted as a distinctive feature in the matrix of low petrologic type ordinary chondrites by Dodd et al. (1967). Nagahara (1984) identified fine-grained (μm-size or less) grains of troilite in the matrix of Semarkona. Brearley (1993) found extremely fine-grained sulfide minerals in the matrix of ALHA77307 and Greshake (1997) reported 100–300 nm Fe, Ni sulfides in the matrix of Acfer 094. It seems likely that most of the S in chondrite matrices and rims is present as sulfide minerals, even in the most primitive chondrites, although those that have experienced aqueous alteration may contain pyrrhotite or pentlandite in addition to troilite (e.g., Alexander et al. 1989; Brearley 1993). Huss et al. (1981) and Nagahara (1984) noted that the sulfide grains in the matrix of primitive ordinary chondrites were coarser in the slightly more metamorphosed ordinary chondrites, some having grain sizes that exceeded those of silicates. The present matrix data confirm this and suggest that the same process affected the matrix in CO chondrites as well.

Mobility of coarse troilite as well as μm-size grains in matrix during metamorphism of ordinary chondrites has also been suggested by Lauretta et al. (1996; 1997), who found experimental evidence for this process, confirmed by textural observations in type 3.3 ALHA76004. Lacy structures such as FeS-rich chondrule rims were probably able to coarsen into more compact grains scattered throughout the chondrite as FeS became mobile during metamorphism and was able to reduce its surface area. Thus, in both chondrule rims and in fine-grained matrix, sulfides became redistributed and coarsened during metamorphism.

The somewhat noisy data presented in Fig. 14c, showing that the FeS abundance in chondrule interiors increases with progressive metamorphism, is not as easily explained. Rubin et al. (1999) found no evidence for a difference in the abundance of primary FeS in chondrules between Semarkona and a range of more metamorphosed type 3 ordinary chondrites. Yet Fig. 14c shows that there is clearly a large range of FeS contents among these same meteorites, without regard to whether the petrographic setting of the grains shows that they are primary or not. The two data sets are thus in conflict.

Coarsening of FeS during metamorphism could result in an increase in the abundance of secondary FeS inside chondrules. The initial state of an unmetamorphosed ordinary chondrite is one in which most of the FeS is in chondrule rims and matrix, with 80 vol% of the rock occupied by chondrules mostly devoid of this phase. Coarsening of the FeS could result in a more even texture as some large grains would form inside chondrules using existing small grains as nuclei.

The very high S content of matrix appears to be a ubiquitous feature of very primitive chondrites such as in type 3.0 ordinary and CO chondrites, as well as in CR and CI chondrites (based on unpublished X-ray maps and literature data), just like the high Cr content of ferroan olivine. Semarkona, the ordinary chondrite with the most S-rich matrix, has considerably less S in its matrix than do ALH A77307, Acfer 094, CR, or CI chondrites. This brings up another key question: is Semarkona more metamorphosed than all of the above-mentioned carbonaceous chondrites, or is there a primary difference between ordinary and carbonaceous chondrites for this parameter? The latter possibility is difficult to assess. The total abundance of S is not very different in Semarkona, Acfer 094, and ALHA77307 (Table 8; Jarosewich 1966; Dreibus et al. 1995; Jarosewich 1990), with Semarkona ~10% lower than the others. Semarkona also contains much less matrix than the other chondrites, which, if anything, might enhance S in its matrix if there is some sort of complementary relationship between chondrules and matrix. There is one line of evidence that Semarkona may have experienced more thermal processing than Acfer 094 and ALHA77307: presolar diamond and SiC abundances are much higher in Acfer 094 (Newton et al. 1995) than in Semarkona (Huss and Lewis 1995), and diamond is higher in ALHA77307 (Huss et al. 2003) than in Semarkona, with SiC being about the same. However, the potential for interlaboratory biases make it difficult to do exact comparisons of presolar grain abundances among these meteorites (Huss, personal communication).

Alkali Mobility in Matrix

The U-shaped relationship between the Na/Al ratio of matrix and the Cr content of ferroan olivine (and therefore metamorphic grade) shown in Fig. 13 indicates that matrix participates in a variety of chemical processes during the early stages of metamorphism. The U-shaped trend is broken only by Bishunpur, which contains matrix with anomalous composition for many elements, possibly due to a high proportion of chondrule debris mixed in the matrix of this highly fragmented and crushed ordinary chondrite (Nelson and Rubin 2002). Using the data from Tables 6 and 7, literature data for bulk compositions (Köblitz 2003), and approximate densities for major components, one can calculate that ~32% of the Na in type 3.0 Semarkona is contained in its matrix. For type 3.2 Krymka, this number falls to only 9%, but by type 3.4 Chainpur 24% of the Na is back in the matrix (in this case, the matrix abundance of 16.1 vol% from Huss et al. [1981] was used in place of the anomalous value of 30 vol% measured in the present work, which is probably due to a nonrepresentative thin section). Bulk Na contents do not show much variation, so the meteorites are probably acting as closed systems. The Na lost

from the matrix between types 3.0 and 3.1 can only go into chondrules, as X-ray maps do not reveal any other alkali-bearing components (like the "white matrix" that is found in Tieschitz; Christophe Michel-Levy 1976; Hutchison et al. 1998). It is likely that type I chondrules are one sink for excess matrix Na at these early stages of metamorphism, resulting in zoned or fully metasomatized chondrules (Grossman et al. 2002). Glass in type II chondrules is another possible sink, as Na/Al does rise in this material in the correct sequence (Fig. 8, Table 5). Because even Semarkona contains zoned chondrules, its matrix must not preserve its original, preaccretionary composition either.

The rise in matrix alkali contents between type 3.1 and higher petrologic types of ordinary chondrites is probably related to secondary crystallization of feldspar in the matrix. With increasing levels of metamorphism, matrix shows increasing levels of blue CL, indicating that feldspar is forming in that location (Sears et al. 1990). The only possible source for the Na that enters matrix is chondrules, possibly the same ones that gained Na during the earliest stages of metamorphism. As discussed above, type II glasses were open to alkali exchange across chondrule borders throughout the metamorphic sequence. There is no clear indication of a drop in the Na/Al ratio of this glass above type 3.1 (Fig. 8, Table 5), although the data are noisy enough to disguise one. Like the feldspar formed inside chondrules by devitrification of glass, we infer that any secondary feldspar that crystallized in the matrix would have a high Na/K ratio (i.e., it was albitic in composition).

The Role of Shock Metamorphism

Impact processing is well known in mobilizing and fractionating alkali elements as well as sulfides (see review by Rubin 1985) and can deposit these elements in melt rocks, veins, and clasts. Heterogeneous alkali distributions attributed to this process have been noted in objects from brecciated and metamorphosed ordinary chondrites (e.g., Ikeda and Takeda 1979; Wlotzka et al. 1983). However, it is unlikely that impact played a direct role in the formation of chondrules containing crystalline albite and fractionated alkali compositions, the redistribution of sulfides, or the exsolution of Cr-rich phases from olivine in the meteorites studied here. All of the analyzed ordinary and CO chondrites have low shock stages, ranging from S1 to S3 on the scale of Stöffler et al. (1991; Table 1) and there is no relationship whatsoever between metamorphic grade and shock stage. There is also little possibility that any of these little-metamorphosed meteorites were shocked to a higher stage and subsequently annealed. Therefore, the various properties of chondrites that correlate well with metamorphic grade are not correlated to shock intensity. This does not mean, however, that shock events elsewhere on the parent body could not have generated the heat or fluids associated with metamorphism in these chondrites.

Classification of Chondrules

DeHart et al. (1992) and Sears et al. (1992) developed a classification scheme for chondrules based on three properties: CL of major phases, especially olivine and mesostasis, CaO-FeO relationships in olivine, and the normative composition of mesostasis. This scheme divides chondrules into two major groups, A (bright CL) and B (low CL), which are in turn divided into subgroups A1–A5 and B1–B3 on the basis of mineral compositions. The large database of mesostasis compositions gathered in the present work offers a chance to re-evaluate a controversial aspect of this system of chondrule classification.

Scott et al. (1994) plotted mesostasis composition for the Semarkona chondrules analyzed by Jones (Jones 1990, 1994, 1996; Jones and Scott 1989) on the normative quartz-anorthite-albite diagram developed for classification purposes by DeHart et al. (1992). Scott et al. observed that many chondrules plotted in the group B2 and B3 fields and almost none plotted in the B1 field, whereas the reverse was true in the DeHart work, which showed many chondrules plotting in the high normative quartz B1 field and few in the other fields. Scott et al. attributed this difference to the fact that Jones used a broad beam to analyze mesostasis, thereby including many crystallites within the glass, whereas DeHart used a 3×3 μm rastered beam in order to avoid crystallites. Sears et al. (1995b) responded to this criticism by showing that results similar to those in DeHart et al. (1992) had been obtained in other labs and re-emphasized that the size of the analyzed region must have been significant due to the presence of quench crystallites.

The present study shows that the data of Scott et al. (1994) are superior to those of DeHart et al. (1992), but not for the reason they thought. Figure 17a shows the DeHart data (taken from DeHart 1989) for Semarkona plotted on their ternary discriminant diagram along with data analyzed in the present study. Our new data differ from both the Jones and the DeHart data by plotting at low normative quartz values; many chondrules are in the A5 and B3 field and few are in the B1 or even the B2 field. The reason for the difference is that the new data are not greatly affected by loss of Na due to electron-beam damage. In the present study, the beam was a factor of 3 less dense than was used by DeHart, analyses were done in the first 10 sec of beam exposure, spots were located using only low magnification imaging, and no significant pre-exposure to electron beams occurred. The effect of not taking these precautions is also plotted on Fig. 17a: the trajectory of analyses of mesostasis in a type II chondrule in which progressively more Na is lost during beam exposure runs from near the albite corner right across the A5, B3, and B2 fields and into the cluster of DeHart analyses in the quartz-rich B1 field. A different diagram also supports the idea that the DeHart analyses are too low in Na (Fig. 17b). As beam damage occurs, mesostasis analyses tend to become

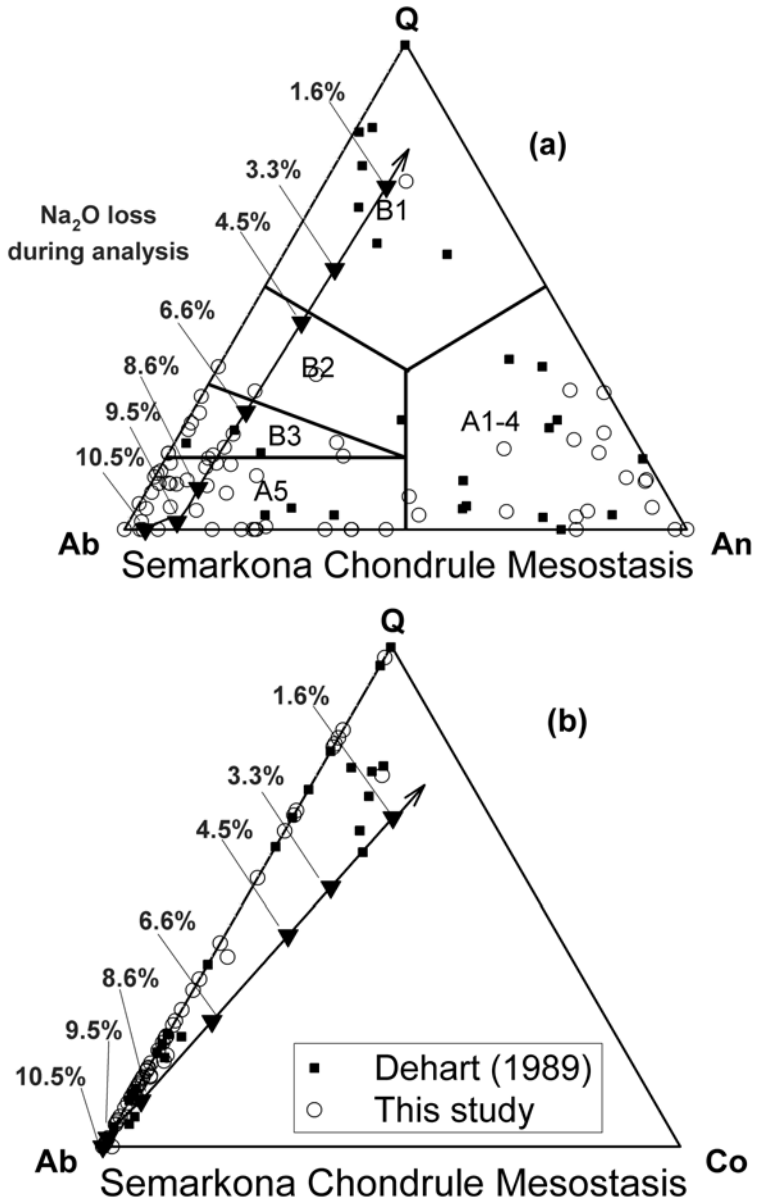

Fig. 17. a) Ternary discriminant diagram for chondrule groups, after DeHart et al. (1992) and Sears et al. (1992), showing the CIPW normative mineral compositions of mesostasis in Semarkona chondrules. Components are Q = quartz, Ab = albite, and An = anorthite. Data from DeHart (1989) (black squares) are compared with those of the present study (open circles). The large inverted triangles, connected by the arrow, show the effect of prolonged exposure to the electron beam of the microprobe on the composition of glass in a type II chondrule. As Na is lost (concentrations are listed at the left), the mesostasis appears to become rich in normative quartz. The B1 field was probably defined on the basis of chondrules that have lost Na during analysis. b) A similar diagram in which normative corundum (Co) replaces anorthite. Loss of Na during analysis results in high normative corundum as well as quartz, a property again shown by chondrules classified as group B1 (cluster near top-center).

progressively richer in normative corundum, an effect seen in all of DeHart's chondrules that plot in the B1 field. Thus, the Jones data are superior to the DeHart data, not because of different amounts of crystallites included in the analysis, but because a less dense electron beam was used, resulting in more accurate Na data.

The consequence of this is that the fields in the ternary discriminant diagram of DeHart et al. (1992) and Sears et al. (1992) delineating A5, B1, B2, B3 are not justified. There probably are real differences between the chondrules that these authors classified as B1 and those that plot in the other fields: these are the chondrules with mesostasis most susceptible to beam damage, meaning that they are chondrules with less crystalline albite. Nevertheless, the discriminant diagram itself should no longer be used.

With increasing levels of metamorphism, increasing

numbers of chondrules in ordinary chondrites show blue CL in their mesostasis. At the same time, induced TL rises in the bulk meteorites. This has long been attributed to progressive devitrification of glass to form sodic feldspars (e.g., Sears et al. 1982; Sears et al. 1990; Sears et al. 1991b; DeHart et al. 1992). The source of blue CL in one chondrule has now been confirmed as crystalline albite, verifying this long line of reasoning. The surprising finding here is that the albite in low type 3 chondrites is not cryptic feldspar resulting from incipient devitrification, but instead large patches of fairly coarse albite are present.

CONCLUSIONS AND FUTURE DIRECTIONS

Ordinary and CO chondrites between types 3.0 and 3.2 show a wide range of metamorphic effects. In addition to those already known, including variations in CL properties of chondrules, differences in the abundances of presolar grains, and changes in opaque mineral assemblages, a series of new parameters has been characterized. These include systematic variations in the Cr content of ferroan olivine, entry of alkalis into the glass of type I chondrules, crystallization of albite from the glass of type II chondrules, changes in alkali content of glass in type II chondrules, variations in the S and Na content of opaque matrix, and changes in the distribution of FeS among different petrographic locations in the meteorites.

The Cr content of ferroan olivine is an extremely sensitive indicator of metamorphic grade in low-petrographic-type chondrites. All of the ferroan olivine in ordinary and carbonaceous chondrites had elevated levels of Cr at the time of accretion, probably a consequence of rapid cooling during chondrule formation. At the onset of metamorphism, Cr rapidly exsolved from olivine, forming fine-grained precipitates probably composed of chromite. Higher degrees of heating caused chromite to coarsen into equant grains inside olivine and form continuous rims around every grain. Cr in olivine is an excellent classification tool for chondrites of types 3.0–3.2 and is not susceptible to modification by aqueous alteration or terrestrial weathering. Differences among the types 3.0 and 3.1 chondrites can be quite large and a further subdivision of petrologic types based on Cr in olivine is proposed to emphasize these differences.

As albite crystallized from type II chondrules during progressive metamorphism, the residual glass changed in composition. At the same time, alkalis entered the glass of type I chondrules. All of these chondrules behaved as open systems during this process, exchanging alkali elements with opaque matrix and probably other chondrules. The secondary albite formed during metamorphism is the source of blue CL, which develops during metamorphism and is also likely responsible for increases in TL sensitivity.

Sulfide Coarsened During Metamorphism

Tiny grains in the matrix coalesced into larger ones at the very earliest stages of heating. Further metamorphism caused FeS-rich rims around chondrules to disappear as coarse matrix grains grew. Sulfides also increased in abundance inside chondrules as the result of metamorphism.

Several ordinary and CO chondrites classified as type 3.0 appear to be more primitive than the others. Among ordinary chondrites, Semarkona is the least metamorphosed of all studied specimens, although the presence of zoned type I chondrules and type II chondrules bearing crystalline albite plus fractionated bulk K/Na indicates that even this meteorite has experienced some heating. The compositions of olivine and matrix in ALHA77307 show it to be less metamorphosed than either Y-81020 or Colony, two other type 3.0s. The ungrouped carbonaceous chondrite Acfer 094 shares many properties with ALHA77307 and is also highly primitive.

Glass in type II chondrules is difficult to analyze and is susceptible to Na loss under an electron beam. This has led to erroneous data in the literature. Almost no chondrules contain highly quartz-normative mesostasis; type II chondrules in primitive meteorites actually contain mesostasis that is highly albitic.

This paper has discussed many metamorphic effects in a relative sense but does not attempt to constrain the actual temperature-time histories of the meteorites. To do this will require a full characterization of the reaction mechanism for Cr exsolution from olivine and experimental work to determine the kinetics of this reaction. Similarly, experimental studies of sulfide mobility, especially with regard to the coalescing of sub-μm grains in opaque matrix, will have the potential to add to the knowledge of chondrite thermal histories.

Acknowledgments–Many discussions with Rhian Jones, Alan Rubin, Conel Alexander, John Wasson, and Bruce Lipin helped us formulate and clarify the ideas presented here. Harvey Belkin provided a huge amount of support in the electron microprobe and SEM aspects of this work. Alan Rubin and Gary Huss provided constructive and helpful reviews. We thank Tim McCoy, Alan Rubin, Gary Huss, Monica Grady, Ted Bunch, Conel Alexander, Addi Bischoff, the National Institute of Polar Research, Tokyo, and the Meteorite Working Group for providing samples to analyze. The first author is grateful to Sorena Sorensen not only for helping with the CL work, but for suffering through endless dinner conversations in which he bombarded her with crazy ideas about the metamorphic petrology of meteorites. This work was supported by NASA's Cosmochemistry Program via order numbers W-10,087 and W-19,575 to J. Grossman. Transmission electron microscopy was performed in the

Electron Microbeam Analysis Facility, Department of Earth and Planetary Sciences, University of New Mexico, a facility supported by the State of New Mexico, NASA, and NSF. Conel Alexander and Chris Hadidiacos generously provided assistance and access to the FE-SEM at the Carnegie Institution of Washington.

Editorial Handling—Dr. Urs Krähenbühl

REFERENCES

Alexander C. M. O., Barber D. J., and Hutchison R. H. 1989. The microstructure of Semarkona and Bishunpur. *Geochimica et Cosmochimica Acta* 53:3045–3057.

Alexander C. M. O. D., Grossman J. N., Wang J., Zanda B., Bourot-Denise M., and Hewins R. H. 2000. The lack of potassium-isotopic fractionation in Bishunpur chondrules. *Meteoritics & Planetary Science* 35:859–868.

Anders E. and Zadnik M. G. 1985. Unequilibrated ordinary chondrites: A tentative subclassification based on volatile-element content. *Geochimica et Cosmochimica Acta* 49:1281–1291.

Armstrong J. T. 1995. CITZAF: A package of correction programs for the quantitative electron microbeam X-ray analysis of thick polished materials, thin films, and particles. *Microbeam Analysis* 4:177–200.

Ashworth J. R. 1979. Two kinds of exsolution in chondritic olivine. *Mineralogical Magazine* 43:535–538.

Benoit P. H., Akridge G. A., Ninagawa K., and Sears D. W. G. 2002. Thermoluminescence sensitivity and thermal history of type 3 ordinary chondrites: Eleven new type 3.0–3.1 chondrites and possible explanations for differences among H, L, and LL chondrites. *Meteoritics & Planetary Science* 37:793–805.

Bonal L., Quirico E., and Bourot-Denise M. 2004. Petrological type of CV3 chondrites as revealed by Raman spectroscopy of organic matter (abstract #1562). 35th Lunar and Planetary Science Conference. CD-ROM.

Brearley A. J. 1993. Matrix and fine-grained rims in the unequilibrated CO3 chondrite, ALHA77307: Origins and evidence for diverse, primitive nebular dust components. *Geochimica et Cosmochimica Acta* 57:1521–1550.

Brearley A. J. and Jones R. H. 1998. Chondritic meteorites. In *Planetary materials*, edited by Papike J. J. Washington, D. C.: Mineralogical Society of America. pp. 313–398.

Chizmadia L. J., Rubin A. E., and Wasson J. T. 2002. Mineralogy and petrology of amoeboid olivine inclusions in CO3 chondrites: Relationship to parent body aqueous alteration. *Meteoritics & Planetary Science* 38:1781–1796.

Christophe Michel-Levy M. 1976. La matrice noire et blanche de la chondrite de Tieschitz (H3). *Earth and Planetary Science Letters* 30:143–150.

DeHart J. M. 1989. Cathodoluminescence and microprobe studies of the unequilibrated ordinary chondrites. Ph.D. thesis, University of Arkansas, Fayetteville, Arkansas, USA.

DeHart J. M., Lofgren G. E., Lu J., Benoit P. H., and Sears D. W. G. 1992. Chemical and physical studies of chondrules X. Cathodoluminescence and phase composition studies of metamorphism and nebular processes in chondrules of type 3 ordinary chondrites. *Geochimica et Cosmochimica Acta* 56: 3791–3807.

Dodd R. T. 1969. Metamorphism of the ordinary chondrites: A review. *Geochimica et Cosmochimica Acta* 33:161–203.

Dodd R. T. 1973. Minor element abundances in olivines of the sharps (H-3) chondrite. *Contributions to Mineralogy and Petrology* 42: 159–167.

Dodd R. T., van Schmus W. R., and Koffman D. M. 1967. A survey of the unequilibrated ordinary chondrites. *Geochimica et Cosmochimica Acta* 31:921–951.

Dreibus G., Palme H., Spettel B., Zipfel J., and Wänke H. 1995. Sulfur and selenium in chondritic meteorites. *Meteoritics* 30: 439–445.

Greshake A. 1997. The primitive matrix components of the unique carbonaceous chondrite Acfer 094: A TEM study. *Geochimica et Cosmochimica Acta* 61:437–452.

Grossman J. N. and Alexander C. M. O. D. 2004. Entry of alkalis into type I chondrules at both high and low temperatures (abstract). *Meteoritics & Planetary Science* 39:A45.

Grossman J. N. and Wasson J. T. 1982. Evidence for primitive nebular components in chondrules from the Chainpur chondrite. *Geochimica et Cosmochimica Acta* 46:1081–1099.

Grossman J. N., Rubin A. E., Nagahara H., and King E. A. 1988. Properties of chondrules. In *Meteorites and the early solar system*, edited by Kerridge J. F. and Matthews M. S. Tucson: The University of Arizona Press. pp. 619–659.

Grossman J. N., Alexander C. M. O. D., Wang J., and Brearley A. J. 2000. Bleached chondrules: Evidence for widespread aqueous processes on the parent asteroids of ordinary chondrites. *Meteoritics & Planetary Science* 35:467–486.

Grossman J. N., Alexander C. M. O. D., Wang J., and Brearley A. J. 2002. Zoned chondrules in Semarkona: Evidence for high- and low-temperature processing. *Meteoritics & Planetary Science* 37:49–73.

Guimon R. K., Symes S. J. K., Sears D. W. G., and Benoit P. H. 1995. Chemical and physical studies of type 3 chondrites XII: The metamorphic history of CV chondrites and their components. *Meteoritics* 30:704–714.

Hewins R. H. 1991. Retention of sodium during chondrule melting. *Geochimica et Cosmochimica Acta* 55:935–942.

Huss G. R. and Lewis R. S. 1994. Noble gases in presolar diamonds II: Component abundances reflect thermal processing. *Meteoritics* 29:811–829.

Huss G. R. and Lewis R. S. 1995. Presolar diamond, SiC, and graphite in primitive chondrites: Abundances as a function of meteorite class and petrologic type. *Geochimica et Cosmochimica Acta* 59: 115–160.

Huss G. R., Keil K., and Taylor G. J. 1981. The matrices of unequilibrated ordinary chondrites: Implications for the origin and history of chondrites. *Geochimica et Cosmochimica Acta* 45: 33–51.

Huss G. R., Meshik A., Kehm K., and Hohenberg C. 1998. Presolar diamonds in Roosevelt County 075 and Axtell: Abundances and noble-gas characteristics (abstract). *Meteoritics & Planetary Science* 33:A72.

Huss G. R., Meshik A. P., Smith J. B., and Hohenberg C. M. 2003. Presolar diamond, silicon carbide, and graphite in carbonaceous chondrites: Implications for thermal processing in the solar nebula. *Geochimica et Cosmochimica Acta* 67:4823–4848.

Huss G. R., Rubin A. E., and Grossman J. N. 2005. Thermal metamorphism in chondrites. In *Meteorites and the early solar system II*, edited by Lauretta D. S., Leshin L. A. and McSween H. Y. Jr. Tucson: The University of Arizona Press.

Hutchison R., Alexander C. M. O., and Barber D. J. 1987. The Semarkona meteorite: First recorded occurrence of smectite in an ordinary chondrite, and its implication. *Geochimica et Cosmochimica Acta* 51:1875–1882.

Hutchison R., Alexander C. M. O. D., and Bridges J. C. 1998. Elemental redistribution in Tieschitz and the origin white matrix. *Meteoritics & Planetary Science* 33:1169–1179.

Ichikawa O. and Ikeda Y. 1995. Petrology of the Yamato-8449 CR chondrite. *Proceedings of the NIPR Symposium on Antarctic Meteorites* 8:63–78.

Ikeda Y. and Takeda H. 1979. Petrology of the Yamato-74442 chondrite. *Proceedings of the Fourth Symposium on Antarctic Meteorites.* pp. 123–139.

Jarosewich E. 1966. Chemical analyses of ten stony meteorites. *Geochimica et Cosmochimica Acta* 30:1261–1265.

Jarosewich E. 1990. Chemical analyses of meteorites: A compilation of stony and iron meteorite analyses. *Meteoritics* 25:323–337.

Johnson C. A. and Prinz M. 1991. Chromite and olivine in type II chondrules in carbonaceous and ordinary chondrites: Implications for thermal history and group differences. *Geochimica et Cosmochimica Acta* 55:893–904.

Jones R. H. 1990. Petrology and mineralogy of type II, FeO-rich chondrules in Semarkona (LL3.0): Origin by closed-system fractional crystallization, with evidence for supercooling. *Geochimica et Cosmochimica Acta* 54:1785–1802.

Jones R. H. 1994. Petrology of FeO-poor, porphyritic pyroxene chondrules in the Semarkona chondrite. *Geochimica et Cosmochimica Acta* 58:5325–5340.

Jones R. H. 1996. FeO-rich, porphyritic pyroxene chondrules in unequilibrated ordinary chondrites. *Geochimica et Cosmochimica Acta* 60:3115–3138.

Jones R. H. and Lofgren G. E. 1993. A comparison of FeO-rich, porphyritic olivine chondrules in unequilibrated chondrites and experimental analogues. *Meteoritics* 28:213–221.

Jones R. H. and Scott E. R. D. 1989. Petrology and thermal history of type IA chondrules in the Semarkona (LL3.0) chondrite. Proceedings, 19th Lunar and Planetary Science Conference. pp. 523–536.

Köblitz J. 2003. MetBase, v. 6.0 for Windows. CD-ROM.

Krot A. N., Zolensky M. E., Wasson J. T., Scott E. R. D., Keil K., and Ohsumi K. 1997. Carbide-magnetite assemblages in type 3 ordinary chondrites. *Geochimica et Cosmochimica Acta* 61:219–237.

Kurat G., Pernicka E., and Herrwerth I. 1984. Chondrules from Chainpur (LL-3): Reduced parent rocks and vapor fractionation. *Earth and Planetary Science Letters* 68:43–56.

Lauretta D. S., Kremser D. T., and Fegley B. 1996. A comparative study of experimental and meteoritic metal-sulfide assemblages. *Proceedings of the NIPR Symposium on Antarctic Meteorites* 9: 97–110.

Lauretta D. S., Lodders K., Fegley B., and Kremser D. T. 1997. The origin of sulfide-rimmed metal grains in ordinary chondrites. *Earth and Planetary Science Letters* 151:289–301.

McCoy T. J., Scott E. R. D., Jones R. H., Keil K., and Taylor G. J. 1991. Composition of chondrule silicates in LL3-5 chondrites and implications for their nebular history and parent body metamorphism. *Geochimica et Cosmochimica Acta* 55:601–619.

McSween H. Y. 1977. Carbonaceous chondrites of the Ornans type: A metamorphic sequence. *Geochimica et Cosmochimica Acta* 41:477–491.

McSween H. Y. and Richardson S. M. 1977. The composition of carbonaceous chondrite matrix. *Geochimica et Cosmochimica Acta* 41:1145–1161.

Merrill G. P. 1921. On metamorphism in meteorites. *Geological Society of America Bulletin* 32:395–416.

Nagahara H. 1984. Matrices of type 3 ordinary chondrites–Primitive nebular records. *Geochimica et Cosmochimica Acta* 48:2581–2595.

Nelson V. E. and Rubin A. E. 2002. Size-frequency distributions of chondrules and chondrule fragments in LL3 chondrites: Implications for parent-body fragmentation of chondrules. *Meteoritics & Planetary Science* 37:1361–1376.

Newton J., Bischoff A., Arden J. W., Franchi I. A., Geiger T., Greshake A., and Pillinger C. T. 1995. Acfer 094, a uniquely primitive carbonaceous chondrite from the Sahara. *Meteoritics* 30:47–56.

Ninagawa K., Hoshikawa Y., Kojima H., Matsunami S., Benoit P. H., and Sears D. W. G. 1998. Thermoluminescence of Japanese Antarctic ordinary chondrite collection. *Antarctic Meteorite Research* 11:1–17.

Rubin A. E. 1985. Impact melt products of chondritic material. *Reviews of Geophysics* 23:277–300.

Rubin A. E., James J. A., Keck B. D., Weeks K. S., Sears D. W. G., and Jarosewich E. 1985. The Colony meteorite and variations in CO3 chondrite properties. *Meteoritics* 20:175–196.

Rubin A. E., Sailer A. L., and Wasson J. T. 1999. Troilite in the chondrules of type 3 ordinary chondrites: Implications for chondrule formation. *Geochimica et Cosmochimica Acta* 63: 2281–2298.

Russell S. S., Folco L., Grady M. M., Zolensky M. E., Jones R., Righter K., Zipfel J., and Grossman J. N. 2004. The Meteoritical Bulletin, No. 88, 2004 July. *Meteoritics & Planetary Science* 39: A215–A272.

Scott E. R. D. and Jones R. H. 1990. Disentangling nebular and asteroidal features of CO3 carbonaceous chondrite meteorites. *Geochimica et Cosmochimica Acta* 54:2485–2502.

Scott E. R. D., Jones R. H., and Rubin A. E. 1994. Classification, metamorphic history, and pre-metamorphic composition of chondrules. *Geochimica et Cosmochimica Acta* 58:1203–1209.

Sears D. W. and Weeks K. S. 1983. Thermoluminescence sensitivity of 16 type 3 ordinary chondrites (abstract). *Lunar and Planetary Science* 14:682–683.

Sears D. W. G., Grossman J. N., Melcher C. L., Ross L. M., and Mills A. A. 1980. Measuring metamorphic history of unequilibrated ordinary chondrites. *Nature* 287:791–795.

Sears D. W. G., Grossman J. N., and Melcher C. L. 1982. Chemical and physical studies of type 3 chondrites-I: Metamorphism related studies of Antarctic and other type 3 ordinary chondrites. *Geochimica et Cosmochimica Acta* 46:2471–2481.

Sears D. W. G., DeHart J. M., Hasan F. A., and Lofgren G. E. 1990. Induced thermoluminescence and cathodoluminescence studies of meteorites. In *Spectroscopic characterization of minerals and their surfaces*, edited by Coyné L. M., McKeever S. W. S. and Blake D. F. Washington, D.C.: American Chemical Society. pp. 190–222.

Sears D. W. G., Batchelor J. D., Lu J., and Keck B. D. 1991a. Metamorphism of CO and CO-like chondrites and comparisons with type 3 ordinary chondrites. *Proceedings of the NIPR Symposium on Antarctic Meteorites* 4:319–343.

Sears D. W. G., Hasan E. A., Batchelor J. D., and Lu J. 1991b. Chemical and physical studies of type 3 chondrites–XI: Metamorphism, pairing, and brecciation of ordinary chondrites. Proceedings, 21st Lunar and Planetary Science Conference. pp. 493–512.

Sears D. W. G., Lu J., Benoit P. H., DeHart J. M., and Lofgren G. E. 1992. A compositional classification scheme for meteoritic chondrules. *Nature* 357:207–210.

Sears D. W. G., Morse A. D., Hutchison R., Guimon R. K., Lu J., Alexander C. M. O. D., Benoit P. H., Wright I., Pillinger C., Xie T., and Lipschutz M. E. 1995a. Metamorphism and aqueous alteration in low petrographic type ordinary chondrites. *Meteoritics* 30:169–181.

Sears D. W. G., Huang S., and Benoit P. H. 1995b. Chondrule formation, metamorphism, brecciation, an important new primary chondrule group, and the classification of chondrules. *Earth and Planetary Science Letters* 131:27–39.

Sorby A. C. 1877. On the structure and origin of meteorites. *Nature* 15:495–498.

Stöffler D., Keil K., and Scott E. R. D. 1991. Shock metamorphism

of ordinary chondrites. *Geochimica et Cosmochimica Acta* 55: 3845–3867.

Sutton S. R., Bajt S., and Jones R. 1996. In situ determination of chromium oxidation state in olivine from chondrules (abstract). 27th Lunar and Planetary Science Conference. pp. 1291–1292.

Van Schmus W. R. and Wood J. A. 1967. A chemical-petrologic classification for the chondritic meteorites. *Geochimica et Cosmochimica Acta* 31:747–765.

Wlotzka F., Palme H., Spettel B., Wänke H., Fredriksson K., and Noonan A. F. 1983. Alkali differentiation in LL-chondrites. *Geochimica et Cosmochimica Acta* 47:743–757.

Wood J. A. 1962. Metamorphism in chondrites. *Geochimica et Cosmochimica Acta* 26:739–749.

Zähringer J. 1968. Rare gases in stony meteorites. *Geochimica et Cosmochimica Acta* 32:209–237.

Zanda B., Bourot-Denise M., Perron C., and Hewins R. H. 1994. Origin and metamorphic redistribution of silicon, chromium and phosphorus in the metal of chondrites. *Science* 265:1846–1849.